Probing Dense Nuclear Matter by Heavy Ion Collisions

Che-Ming Ko
Texas A&M University

- Introduction
- High energy collisions and nuclear equation of state
- Collisions with neutron-rich nuclei and nuclear symmetry energy
- Collisions at ultrarelativistic energies and quark-gluon plasma
- Conclusions

Supported by National Science Foundation and The Welch Foundation

Siu A. Chin's seminar contributions to the physics of dense nuclear matter

- An equation of state of nuclear and high-density matter based on a relativistic mean-field theory, Phys. Lett. B 52, 24 (1974)
- A relativistic many-body theory of high density matter, Ann. Phys. 108, 301 (1977)

to relativistic heavy ion collisions

- Transition to hot quark matter in relativistic heavy ion collision, Phys. Lett B 78, 552 (1978)
- Dilepton production from hot quark matter in an ultrarelativistic heavy ion collision, Phys. Lett. B 119, 51 (1982)

and to nuclear astrophysics

- Can a neutron star be a giant MIT bag, Phys. Lett. B 62, 241 (1976)
- Possible long-lived hyperstrange multi-quark droplet, Phys. Rev. Lett. 43, 1292 (1979)

Equation of state of nuclear and neutron matter

Fuchs, JPG 35, 014049 (2008)

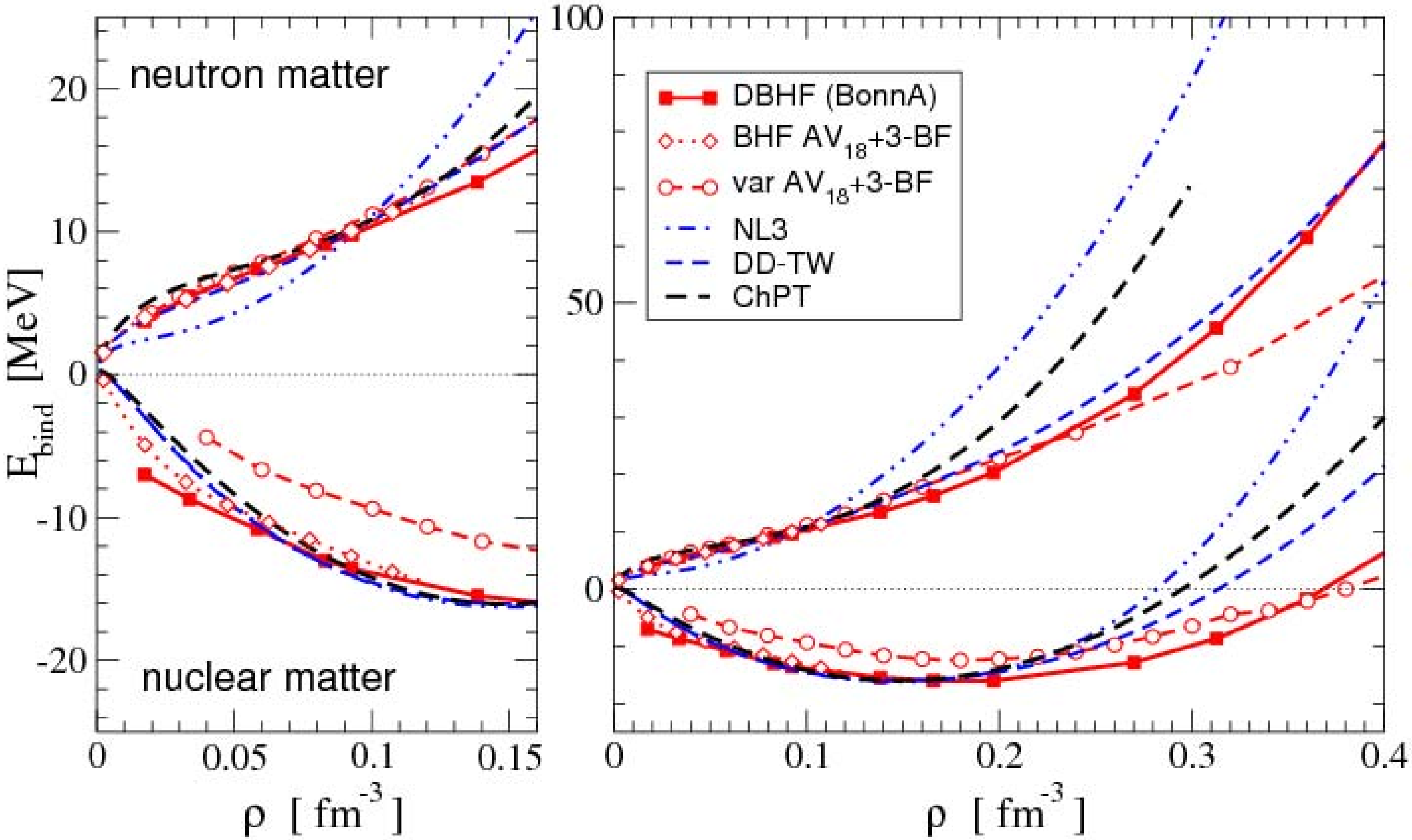

Large uncertainties at both low and high densities

Nuclear symmetry energy

Li, Chen & Ko, Phys. Rep. 464, 113 (2008)

EOS of asymmetric nuclear matter

$$E(\rho,\delta) \approx E(\rho,\delta=0) + E_{sym}(\rho)\delta^2, \quad \delta = \frac{\rho_n - \rho_p}{\rho_n + \rho_p}$$

Symmetry energy
$$E_{sym}(\rho) = E_{sym}(\rho_0) + \frac{L}{3}\left(\frac{\rho-\rho_0}{\rho_0}\right) + \frac{K_{sym}}{18}\left(\frac{\rho-\rho_0}{\rho_0}\right)^2$$

Symmetry energy coefficient
$$E_{sym}(\rho_0) \approx 30\ \mathrm{MeV}$$

Slope
$$L = 3\rho_0 \left.\frac{\partial E_{sym}(\rho)}{\partial\rho}\right|_{\rho=\rho_0}$$
theoretical values -50 to 200 MeV

Curvature
$$K_{sym} = 9\rho_0^2 \left.\frac{\partial^2 E_{sym}(\rho)}{\partial^2\rho}\right|_{\rho=\rho_0}$$
theoretical values -700 to 466 MeV

Nuclear matter Incompressibility
$$K(\delta) = K_0 + K_{asy}\delta^2, \quad K_{asy} \approx K_{sym} - 6L$$

Empirically,
K_0~ 230±10 MeV, K_{asy}~ -500 ±50 MeV, L~ 88±50 MeV

$E_{sym}(\rho)$~ 32 $(\rho/\rho_0)^\gamma$ with $0.7<\gamma<1.1$ for $\rho<1.2\rho_0$

Symmetry energy at high densities is practically undetermined !

Theoretical predictions on nuclear symmetry energy

Fuchs, JPG 35, 014049 (2008)

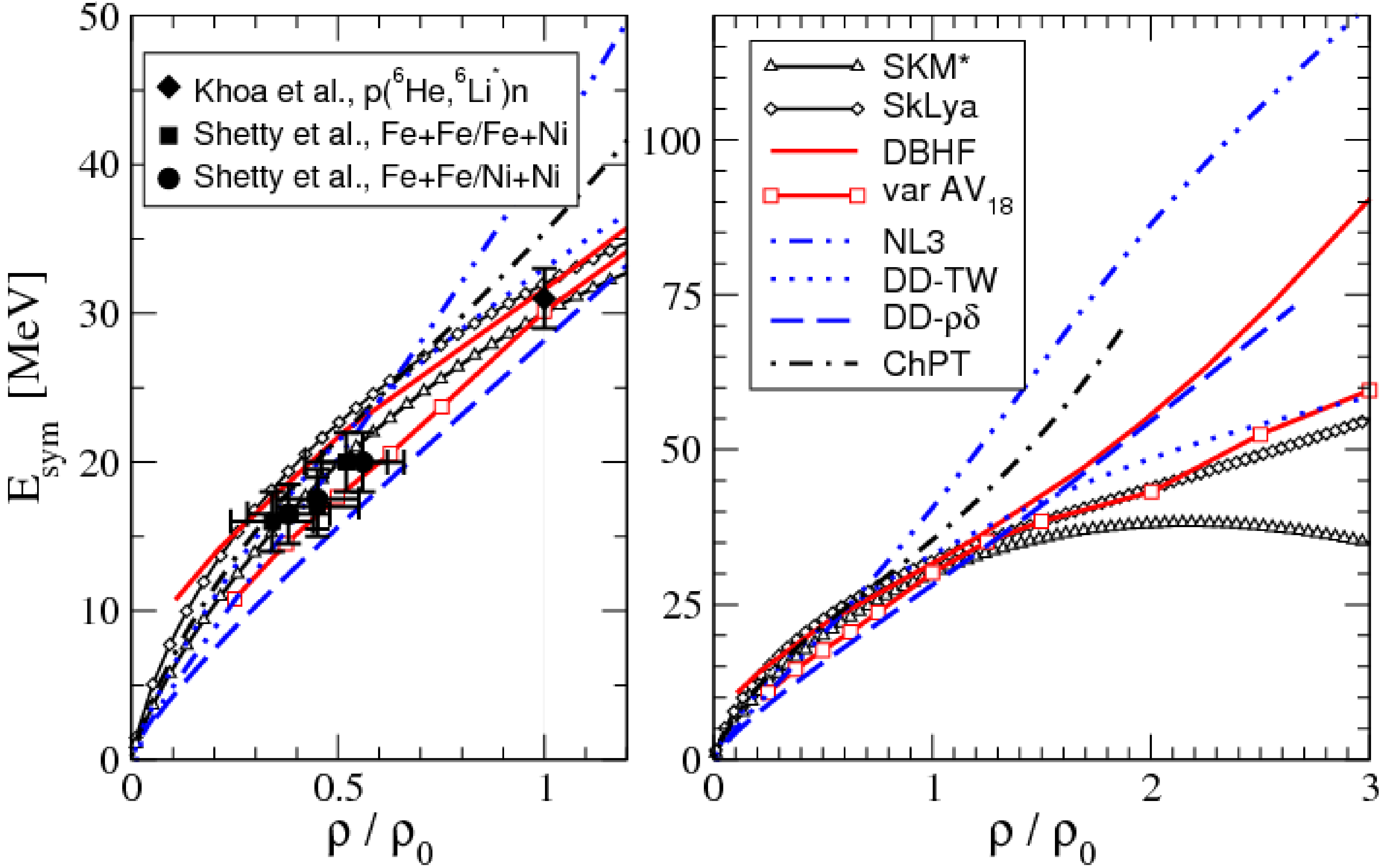

Large uncertainties at both low and high densities

QCD equation of state

Karsch et al., NPA 698, 199 (02)

Lattice QCD

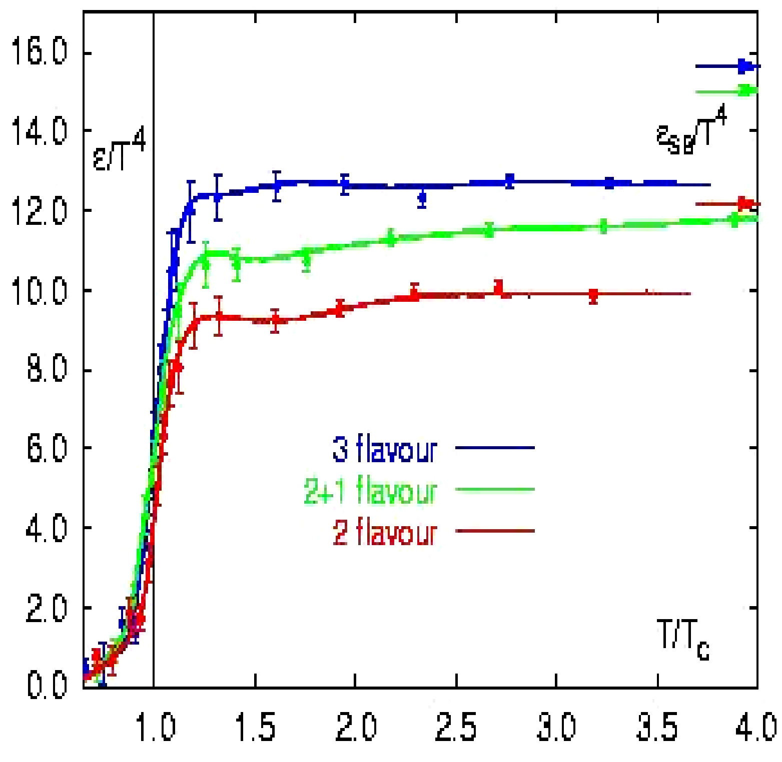

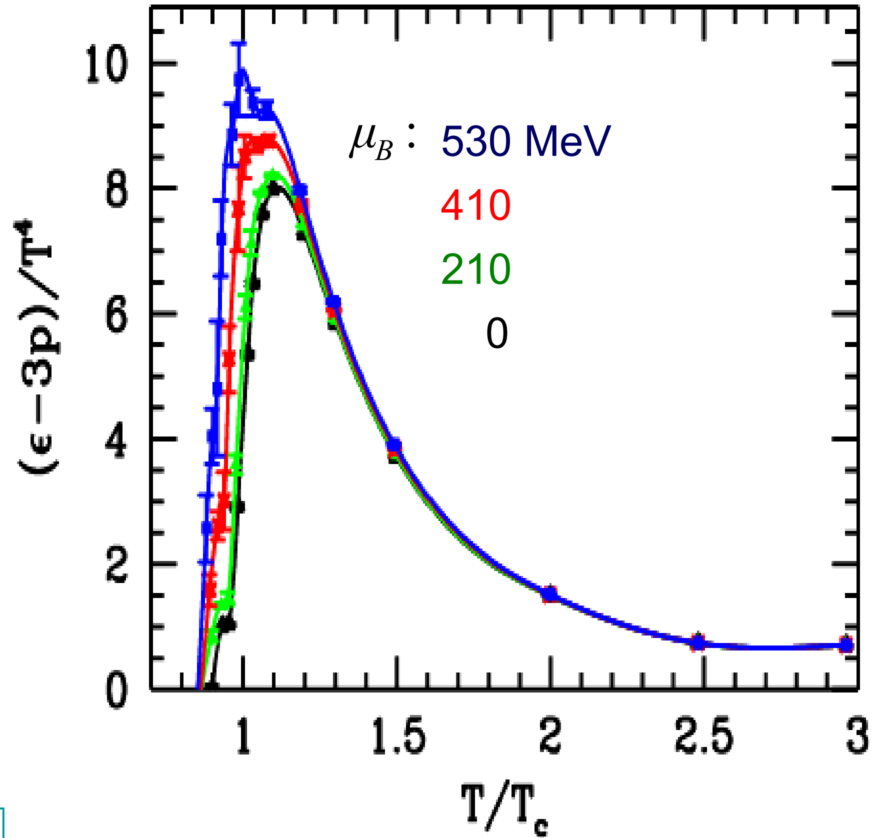

- Soft equation of state (p< e/3)
- $e_c \sim 6T_c^4 \sim 0.66$ GeV/fm^3
- Appreciate interaction energy
- $T_c \sim 170$ MeV

$$\frac{\varepsilon_{SB}}{T^4} = \left(16 + \frac{21}{2} n_f\right)\frac{\pi^2}{30}, \quad \frac{\varepsilon_\pi}{T^4} = 3\frac{\pi^2}{30}$$

Evolution of nuclear density in HI collisions

Li & Ko, NPA 601, 269 (1996)

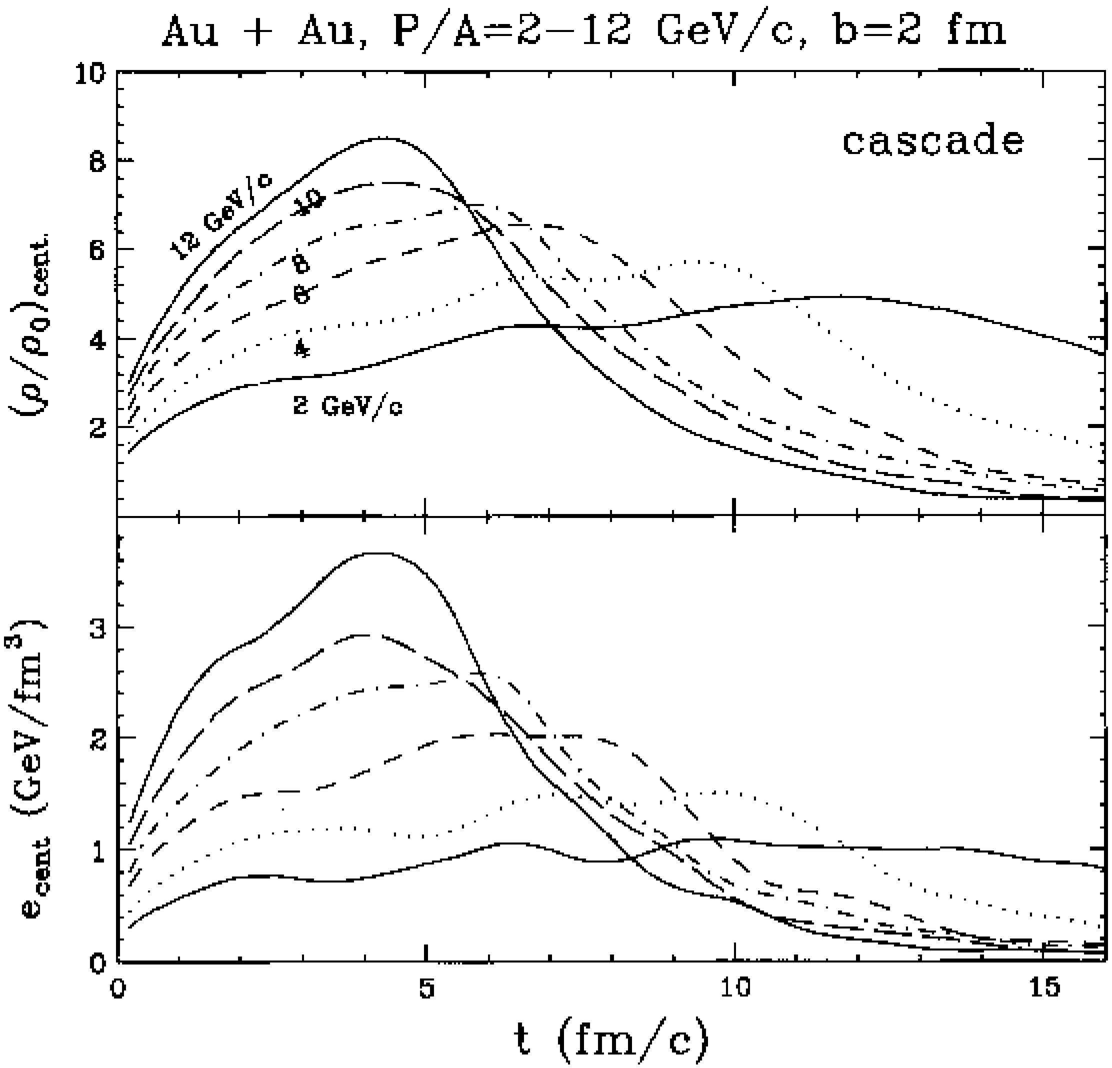

Mapping QCD phase diagram via heavy ion collisions

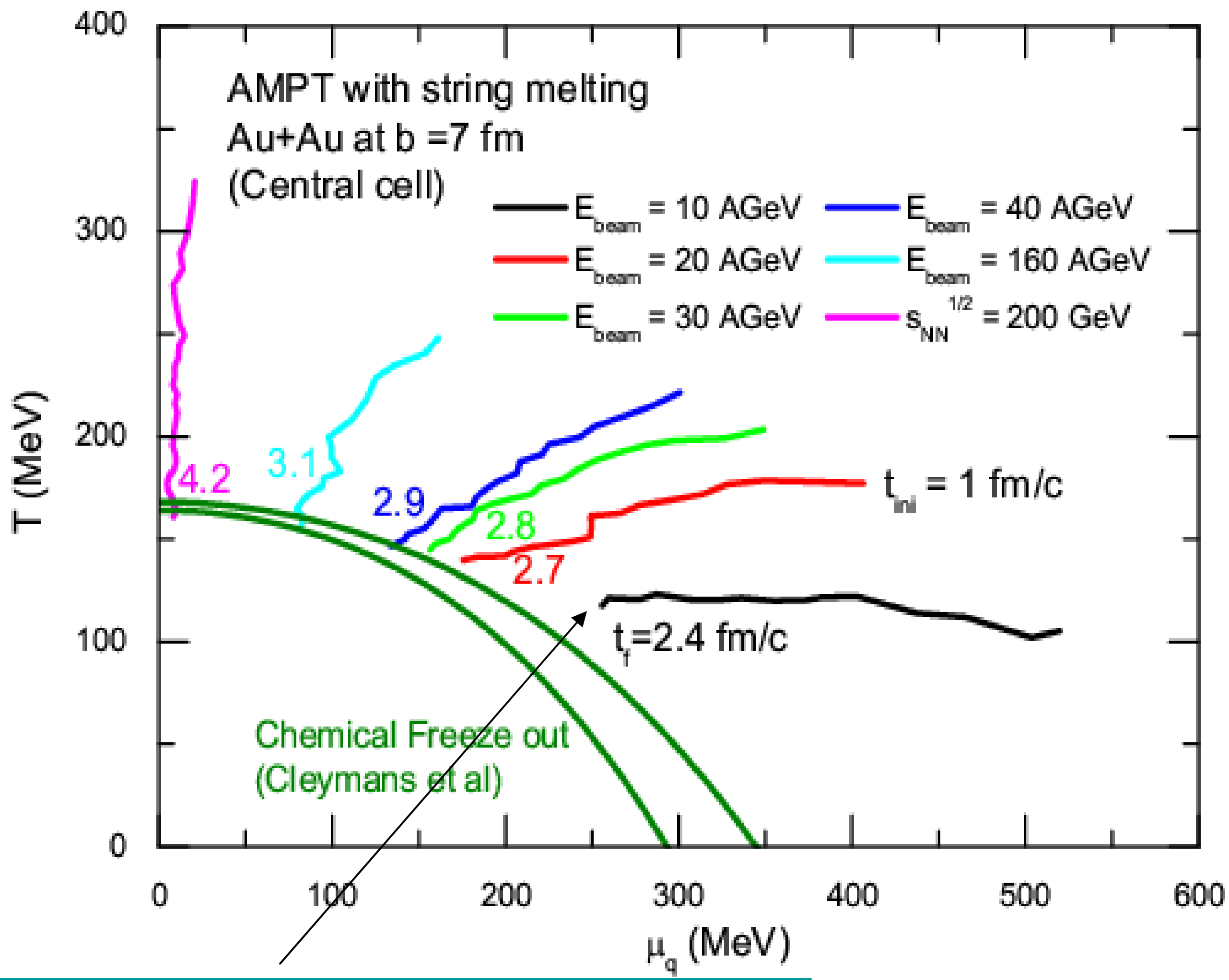

Require first-order phase transition ?

Chronology of heavy ion collisions

- 1970's: below Coulomb barrier → deeply inelastic collisions;
  nuclear dissipation and damping of collective motions
- 1980's: high energies (~1-2 GeV/nucleon @ fixed target, Bevalac);
  nuclear equation of state at high densities ($\sim 3\rho_0$)
- 1990's: high (GSI) and relativistic (~10-100 GeV/nucleon @ fixed target, AGS, SPS);
  nuclear equation of state ($\sim 5\rho_0$) and quark-gluon plasma
- 2000's: ultrarelativistic energies (~100 GeV/nucleon @ c.m., RHIC)
  → nearly baryon-free quark-gluon plasma;
  neutron-rich nuclei (MSU,GSI) → nuclear symmetry energy ($\sim\rho_0$)
- 2010's: ultrarelativstic energies (~5 TeV/nucleon @ c.m., LHC)
  → baryon-free quark-gluon plasma
- 2020's: relativistic energies (~10 GeV/nucleon @ c.m., FAIR)
  → baryon-rich quark-gluon plasma;
  medium energies (~400 MeV/nucleon @ fixed target, FRIB)
  → nuclear symmetry energy ($\sim 2.5\rho_0$)

Boltzmann-Uehling-Uhlenbeck model

Bertsch &Das Gupta, Phys. Rep. 160, 189 (1988)

$$
\begin{aligned}
&\frac{\partial f(r,p,t)}{\partial t} + v \cdot \nabla_r f - \nabla_r U \cdot \nabla_p f = \left(\frac{\partial f}{\partial t}\right)_{coll} \\
&= -\frac{1}{(2\pi)^3} \iint dp_2 dp_3 \int d\Omega \left| v_{12} \right| \frac{d\sigma}{d\Omega}(p_2 - p_4)\delta(p + p_2 - p_3 - p_4) \\
&\quad \times \{ f(r,p_3,t) f(r,p_4,t)[1 - f(r,p,t)][1 - f(r,p_2,t)] \\
&\quad - f(r,p,t) f(r,p_2,t)[1 - f(r,p_3,t)][1 - f(r,p_4,t)] \}
\end{aligned}
$$

- F(r,p,t): nucleon distribution function
- U(r): nuclear mean-field potential
  e.g., Skyrme potential U=α ρ(r) + β $\rho^{4/3}$(r)
- dσ/dΩ: nucleon-nucleon scattering cross sections

Collective flow in heavy ion collisions

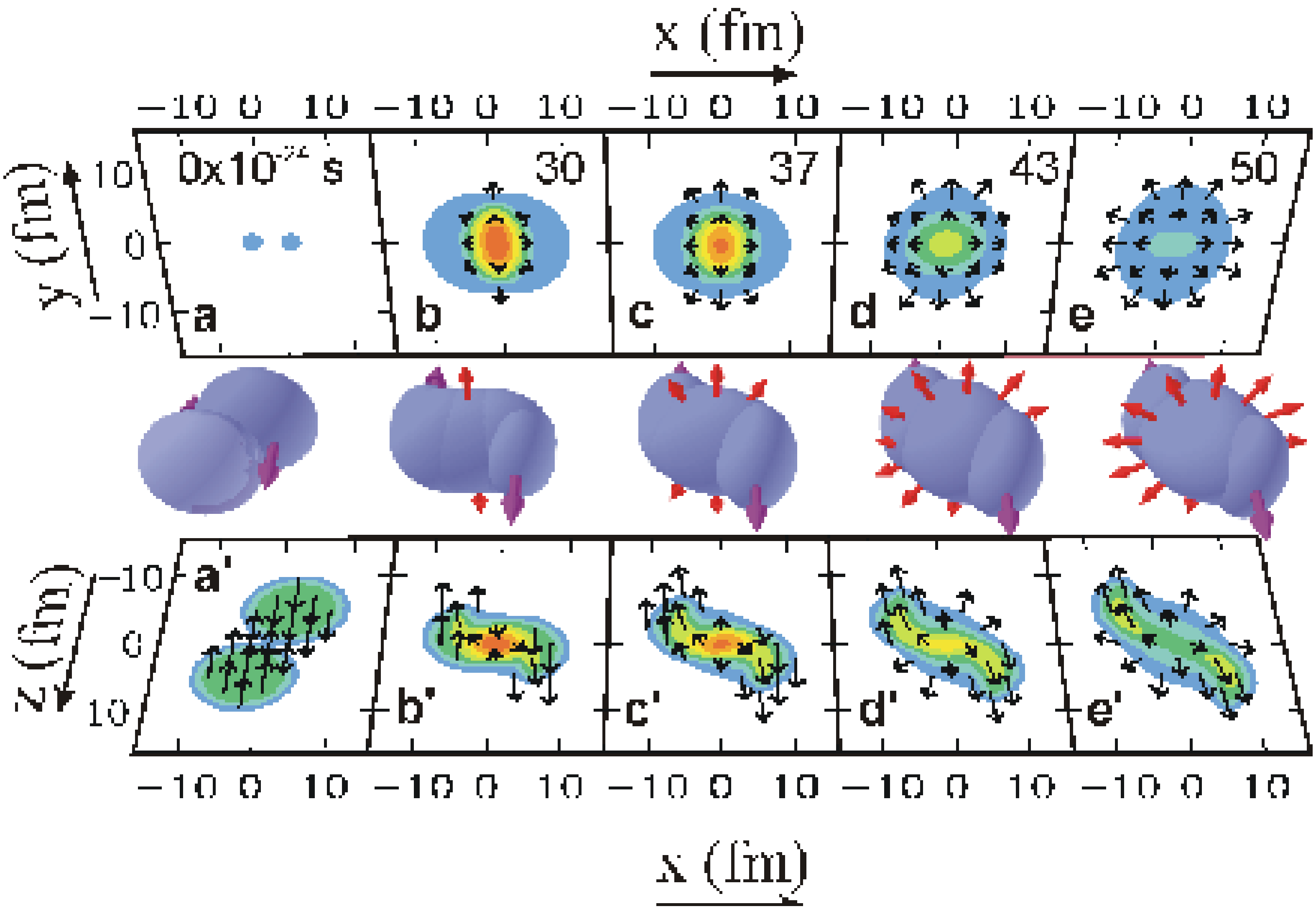

Directed flow in the reaction (x-z) plane and elliptic flow in the transverse (x-y) plane.

Danielewicz, Lacey & Lynch, Science 298, 1592 (2002)

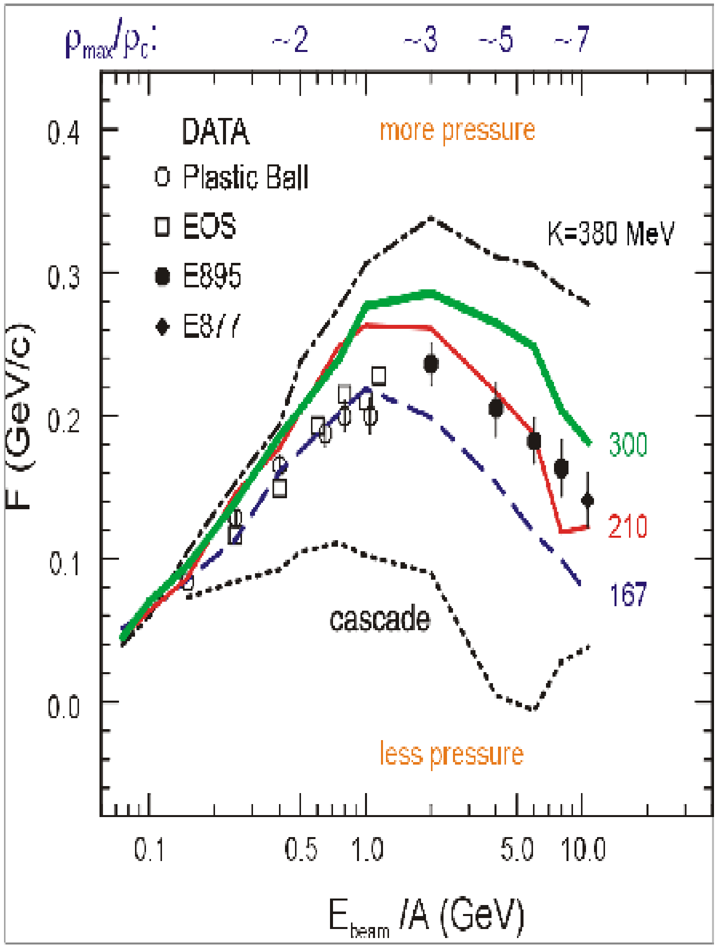

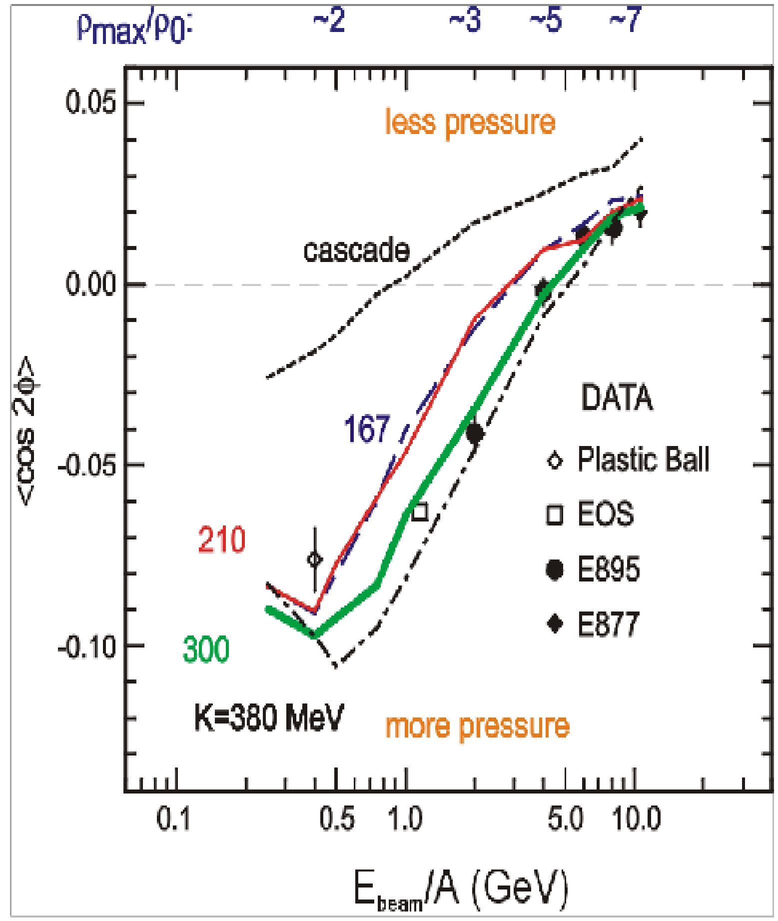

Direct flow $F = \left(\frac{dp_x}{dy} \right)_{y_{cm}}$

Elliptic flow $v_2 = \langle \cos 2\varphi \rangle = \left\langle \frac{p_x^2 - p_y^2}{p_x^2 + p_y^2} \right\rangle$

Subthreshold kaon production

Aichelin & Ko, PRL 55, 2661 (85)

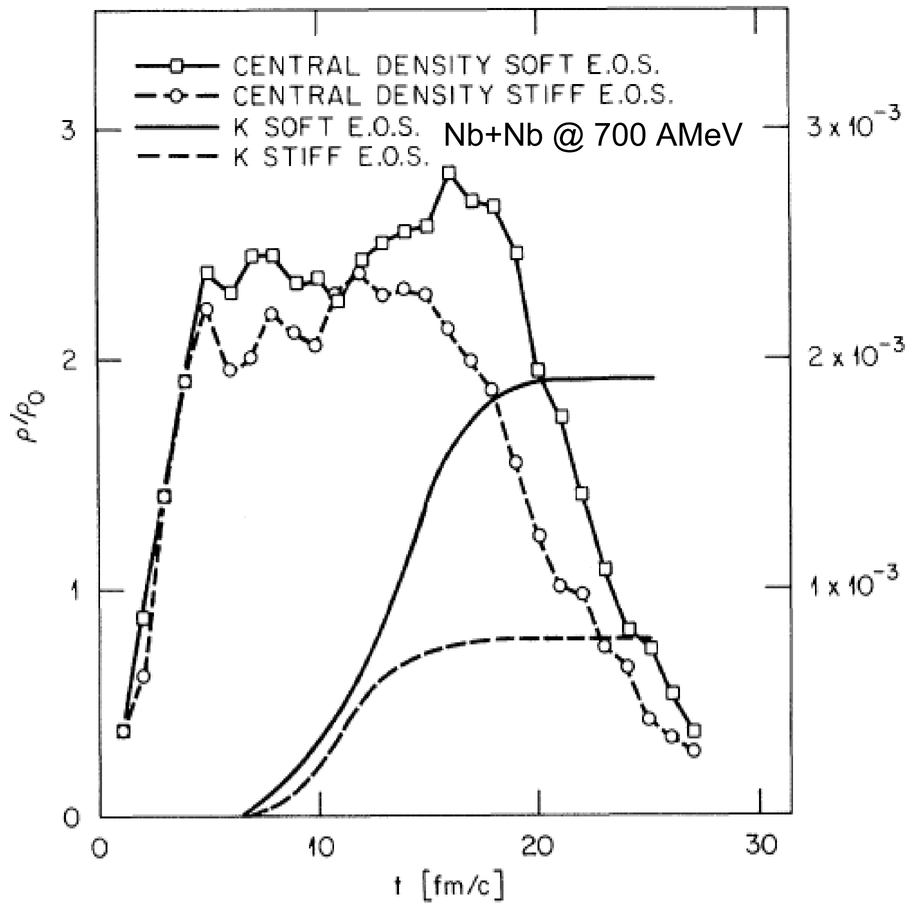

Fuchs, PRL 86, 1974 (2001)

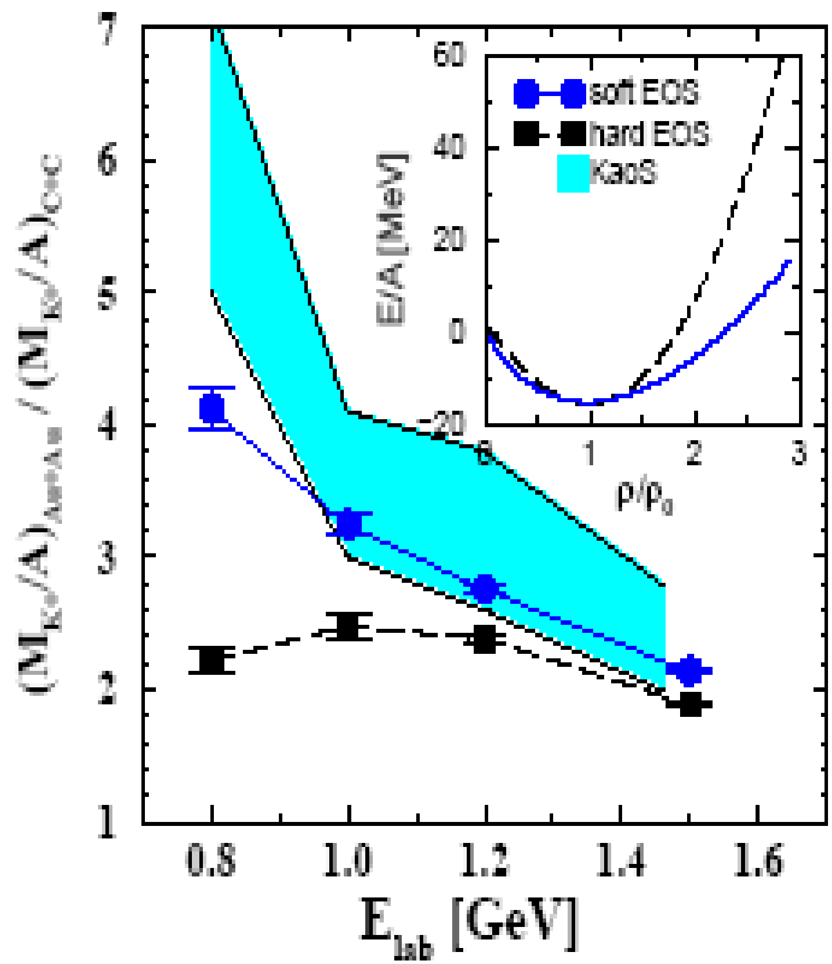

Kaon production at subthreshold energy in HI collisions is sensitive to nuclear EOS and data are consistent with a soft one.

Isospin-dependent transport model (IBUU)

$$\frac{\partial f(\vec{r},\vec{p},t)}{\partial t}+\vec{v}\cdot\vec{\nabla}_r f-\vec{\nabla}_r U\cdot\vec{\nabla}_p f=I_c(f,\sigma_{NN})$$

- Mean-field potential from the HF approach using a modified Gogny force

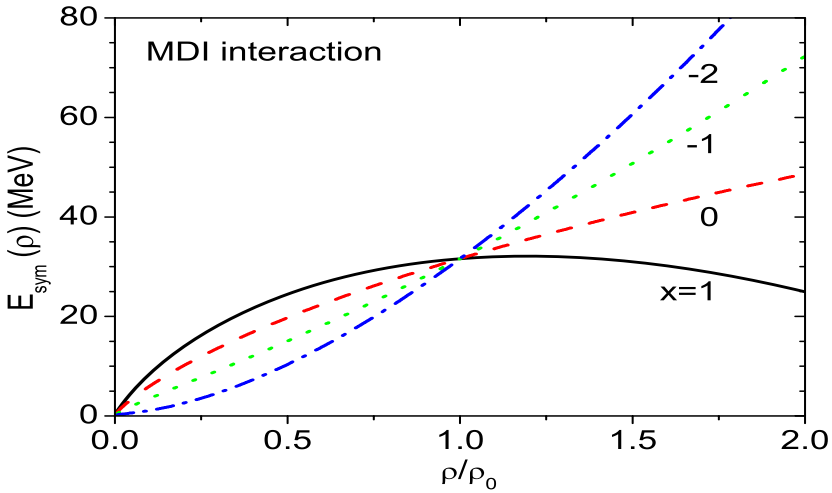

The x parameter is introduced to mimic various predictions by different microscopic nuclear many-body theories using different effective interactions

$$U(\rho,\delta,\vec{p},\tau,x)=A_u(x)\frac{\rho_{\tau'}}{\rho_0}+A_l(x)\frac{\rho_\tau}{\rho_0}+B\left(\frac{\rho}{\rho_0}\right)^\sigma(1-x\delta^2)-8\tau x\frac{B}{\sigma+1}\frac{\rho^{\sigma-1}}{\rho_0^\sigma}\delta\rho_{\tau'}$$
$$+\frac{2C_{\tau,\tau}}{\rho_0}\int d^3p'\frac{f_\tau(r,p')}{1+(p-p')^2/\Lambda^2}+\frac{2C_{\tau,\tau'}}{\rho_0}\int d^3p'\frac{f_{\tau'}(r,p')}{1+(p-p')^2/\Lambda^2}$$
$$\tau,\tau'=\pm\frac{1}{2},\ A_l(x)=-121+\frac{2Bx}{\sigma+1},\ A_u(x)=-96-\frac{2Bx}{\sigma+1},\ K_0=211MeV$$

Isospin diffusion in heavy ion collisions

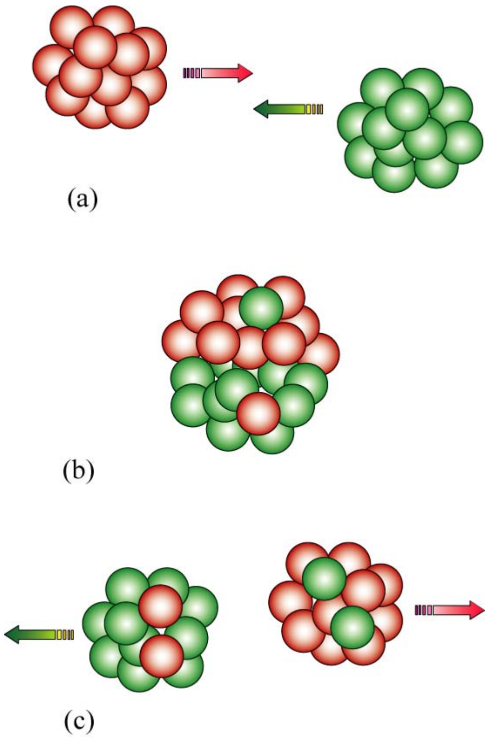

F. Rami et al. (FOPI/GSI), PRL 84, 1120 (2000)

For any isospin-sensitive observable, a quantitative measure of isospin transport is

$$R_X^{A+B} \equiv \frac{2X^{A+B} - X^{A+A} - X^{B+B}}{X^{A+A} - X^{B+B}}$$

$$R_X^{A+A} = 1 \text{ and } R_X^{B+B} = -1$$

$$R_X^{A+B} \approx 0$$ for complete isospin mixing

The degree of isospin transport/diffusion depends on both the symmetry potential and the in-medium neutron-proton scattering cross section.

Isospin transport/diffusion:

$$\Gamma_n - \Gamma_p \propto \rho D_I \nabla_r \delta$$

$$\frac{\partial \delta}{\partial t} = D_I \nabla^2 \delta$$

L. Shi and P. Danielewicz, PRC68, 064604 (2003)

For near-equilibrium systems, the mean-field contributes

$$D_I^m \propto \frac{\partial}{\partial \delta}[\mu_n - \mu_p + U_n - U_p] \propto [4E_{sym}(\rho) + 2U_{sym}(\rho, p)]$$

During heavy-ion reactions, the collisional contribution to D_I is expected to be proportional to σ_{np}

Transport model analysis of the NSCL/MSU isospin data

L.W. Chen, C.M. Ko and B.A. Li, Phys. Rev. Lett 94, 32701 (2005)
B.A. Li and L.W. Chen, Phys. Rev. C72, 064611 (2005)

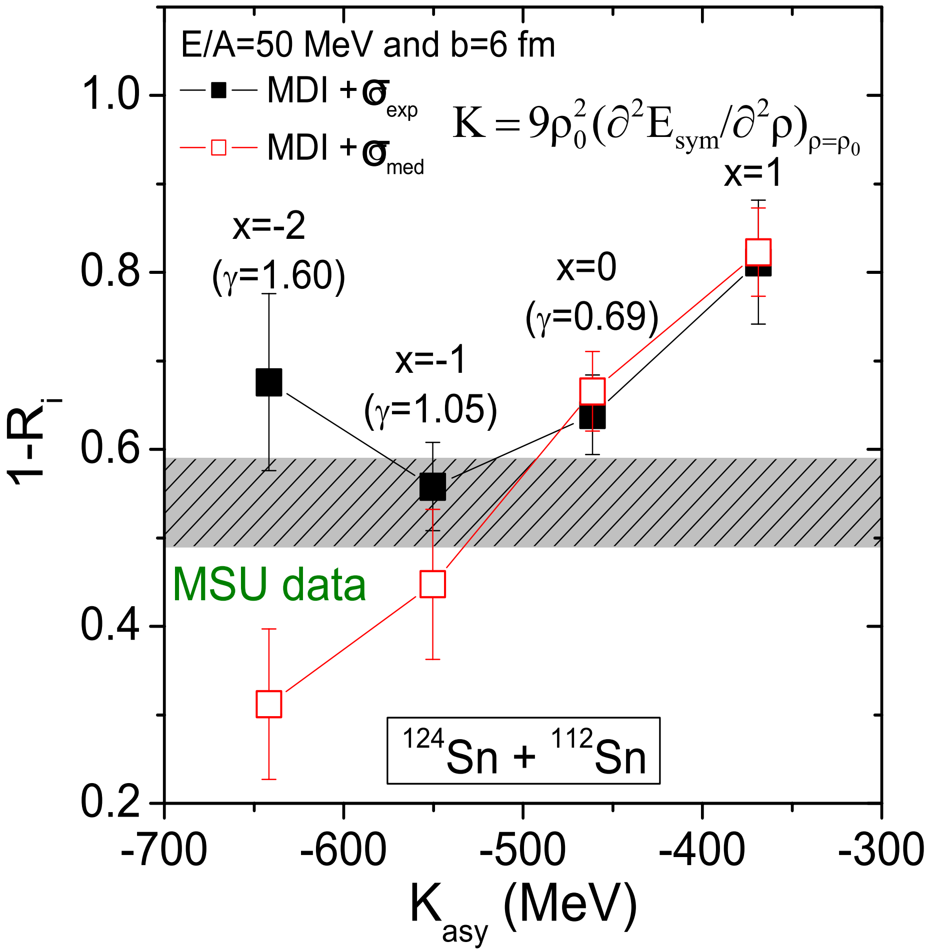

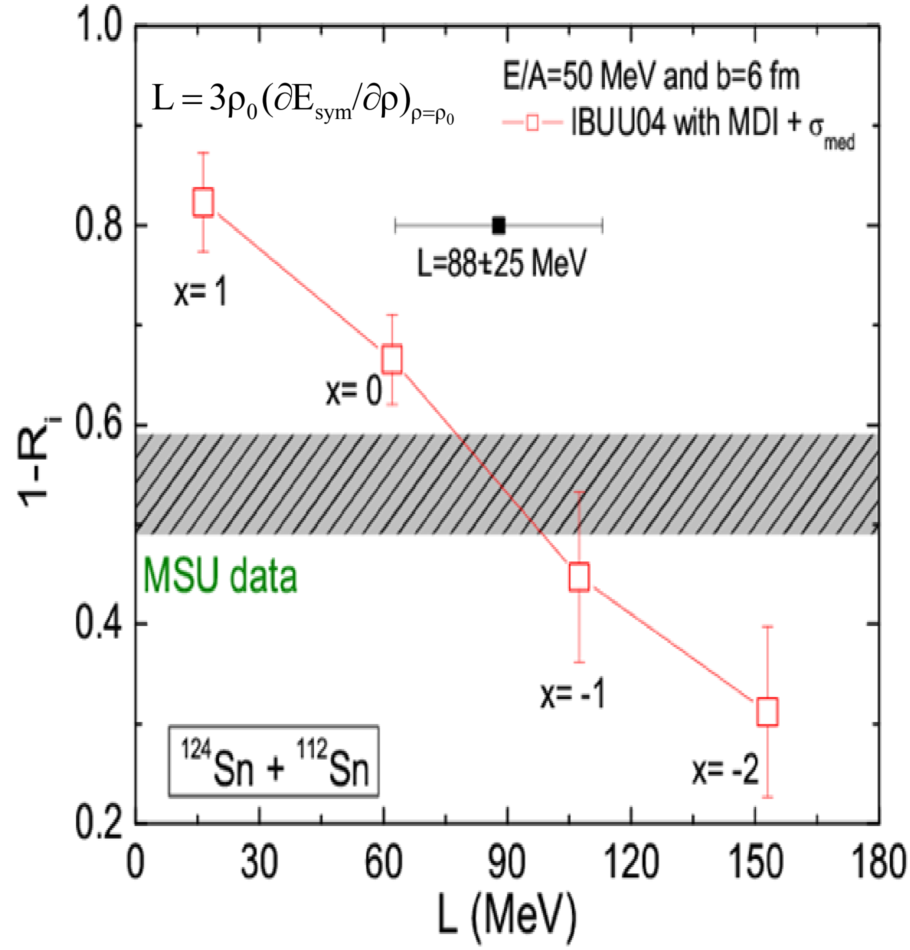

$E_{sym}(\rho) \sim 32\ (\rho/\rho^0)^\gamma$ with $0.7<\gamma<1.1$ for $\rho<1.2\rho_0$
$\rightarrow K_{asy}(\rho_0) \sim -550 \pm 50$ MeV and $L \sim 88 \pm 25$ MeV

Nuclear equation of state

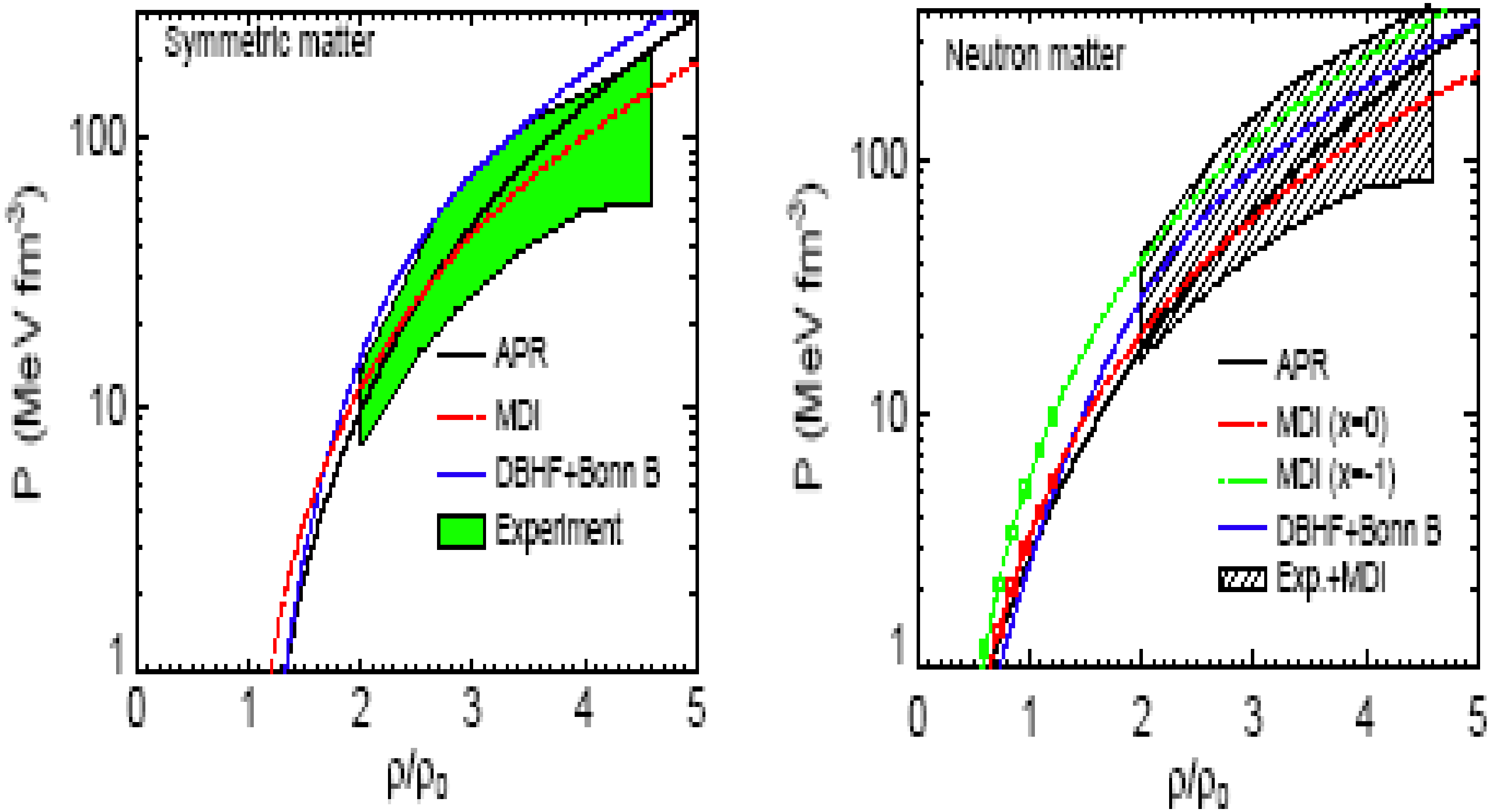

Constraints for symmetric nuclear matter from flow data while those for asymmetric nuclear matter from isospin diffusion data

Time evolution of a RHIC event at 130G

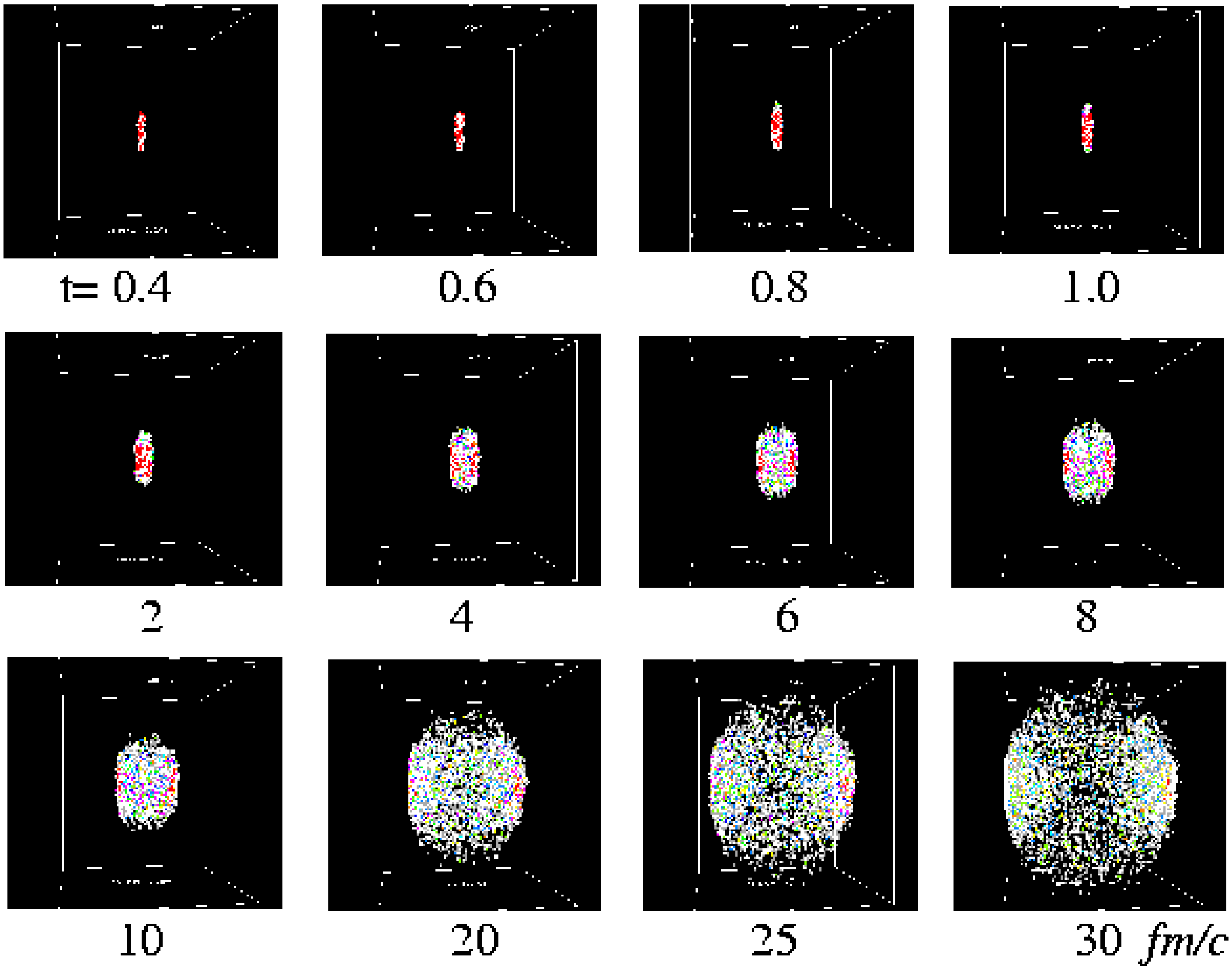

A quark-gluon plasma is expected to be produced during initial stage

Statistical model

Braun-Munzinger et al.

Assume thermally and chemically equilibrated system of non-interacting hadrons and resonances with density

$$n_i = \frac{g}{2\pi^2}\int_0^\infty \frac{p^2 dp}{e^{(E_i(p)-\mu_i)/T} \pm 1}, \quad E_i = \sqrt{p^2 + m_i^2}$$

Determine chemical freeze out temperature T_{ch} and baryon chemical potential μ_B by fitting experimental data after inclusion of feed down from short lived particles and resonances decay.

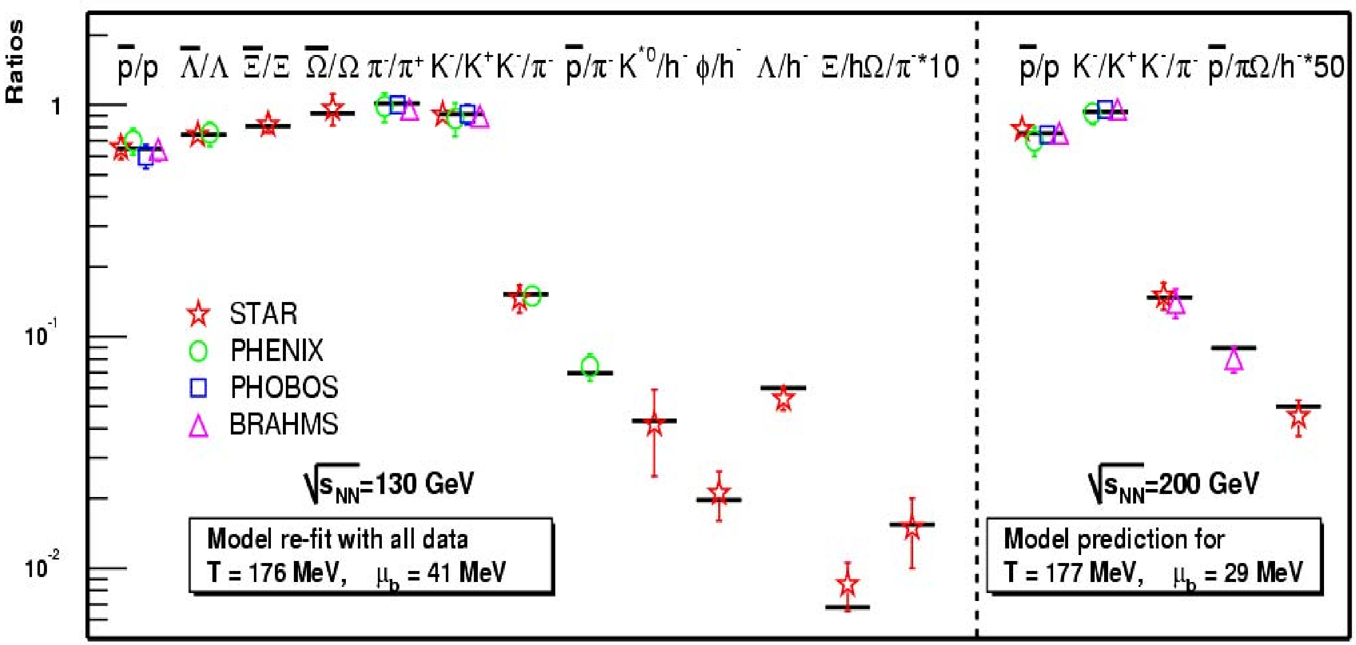

$\boxed{T_{ch} \sim T_c}$

Hydrodynamic model

Kolb & Heinz; Teany & Shuryak; Hirano, ……..

Hydrodynamic Equations

$$\partial_\mu T^{\mu\nu}(x) = 0$$ Energy-momentum conservation

$$\partial_\mu n_j u^\mu(x) = 0$$ Charge conservations (baryon, strangeness,…)

For perfect fluids without viscosity

$$T^{\mu\nu}(x) = [e(x) + p(x)]u^\mu(x)u^\nu(x) - p(x)g^{\mu\nu}$$

e: energy density
p: pressure
u^μ: four velocity

Equation is closed by the equation of state p(e)

Cooper-Frye instantaneous freeze out

$$\boxed{E\frac{dN_i}{d^3q} = \frac{g_i}{(2\pi 2^3}\int q\cdot d\sigma \frac{1}{\exp(q\cdot u)\pm 1}}$$

dσ is an element of space-like hypersurface

Elliptic flow from hydrodynamic model

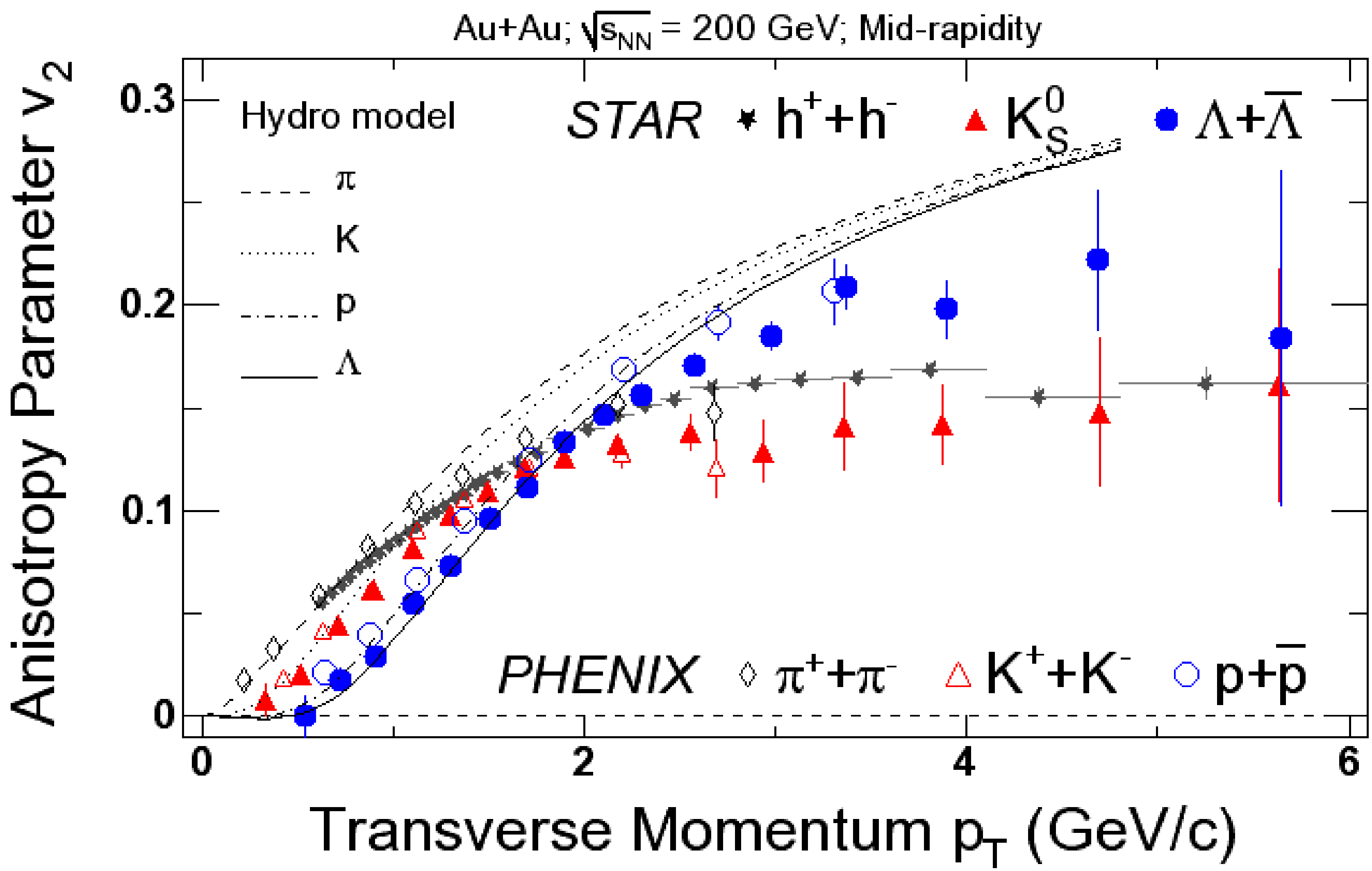

Ideal hydro describes very well data at low p_T (mass effect) but fails at intermediate p_T → viscous or nonequlibrium effect

Parton cascade

Bin Zhang, Comp. Phys. Comm. 109, 193 (1998)
D. Molnar, B.H. Sa, Z. Xu & C. Greiner

$$p^{\mu}\,\partial_{\mu} f_1(x,p,t) \propto \int dp_2 d\Omega \left|\vec{v}_1 - \vec{v}_2\right| \frac{d\sigma}{d\Omega}\left(f_1' f_2' - f_1 f_2\right)$$

$$\frac{d\sigma}{dt} \approx \frac{9\pi\alpha_s^2}{2(t - \mu^2)^2}, \qquad \sigma = \frac{9\pi\alpha_s^2}{2\mu^2}\frac{1}{1+\mu^2/s}$$

- Using α_s=0.5 and screening mass μ=gT≈0.6 GeV at T≈0.25 GeV, then $\langle s\rangle^{1/2}$≈4.2T≈1 GeV, and pQCD gives σ≈2.5 mb and a transport cross section

$$\sigma_t \equiv \int d\Omega \frac{d\sigma}{d\Omega}\left(1 - \cos\theta\right) \approx 1.5\,\mathrm{mb}$$

- σ=6 mb → μ≈0.44 GeV, σ_t≈2.7 mb
- σ=10 mb → μ≈0.35 GeV, σ_t≈3.6 mb

Elliptic flow from Zhang's parton cascade

Zhang, Gyulassy & Ko, PLB 455, 45 (1999)

Based on Zhang's parton cascade (ZPC) (CPC 109, 193 (1998)), using minijet partons from HIJING for Au+Au @ 200 AGeV and b=7.5fm

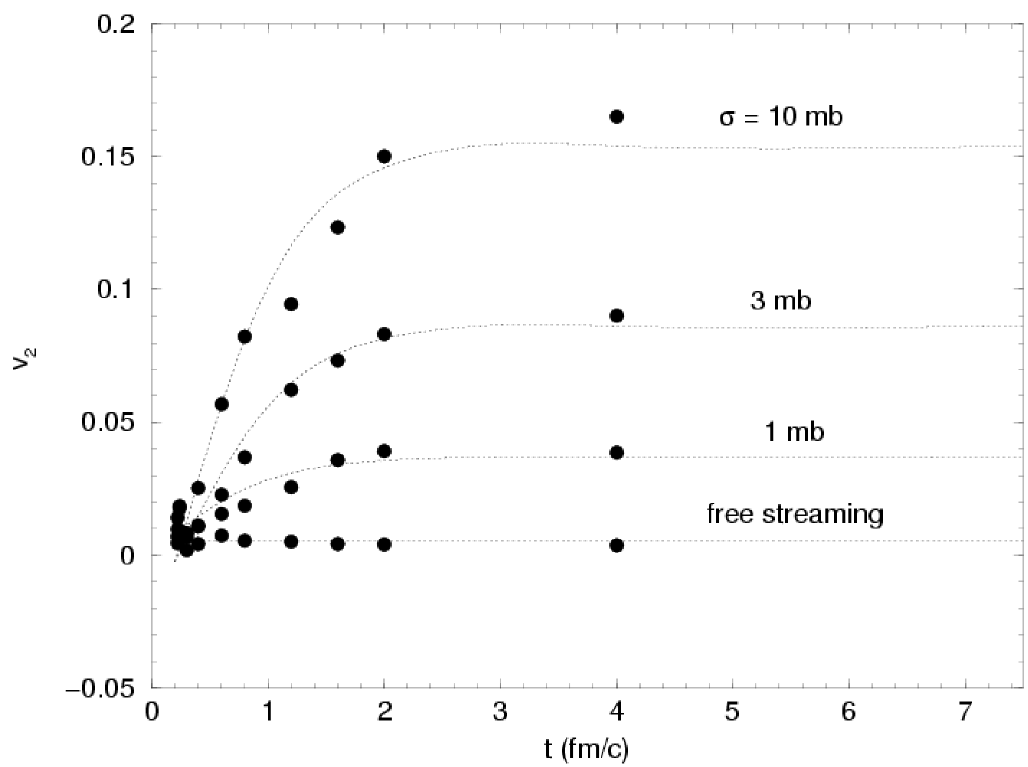

v_2 of partons is sensitive to their scattering cross section

A multiphase transport (AMPT) model

Default: Lin, Pal, Zhang, Li & Ko, PRC 61, 067901 (00); 64, 041901 (01); 72, 064901 (05); http://www-cunuke.phys.columbia.edu/OSCAR

- Initial conditions: HIJING (soft strings and hard minijets)
- Parton evolution: ZPC
- Hadronization: Lund string model for default AMPT
- Hadronic scattering: ART

String melting: PRC 65, 034904 (02); PRL 89, 152301 (02)

- Convert hadrons from string fragmentation into quarks and antiquarks
- Evolve quarks and antiquarks in ZPC
- When partons stop interacting, combine nearest quark and antiquark to meson, and nearest three quarks to baryon (coordinate-space coalescence)
- Hadron flavors are determined by quarks' invariant mass

Elliptic flow from AMPT

Lin & Ko, PRC 65, 034904 (2002)

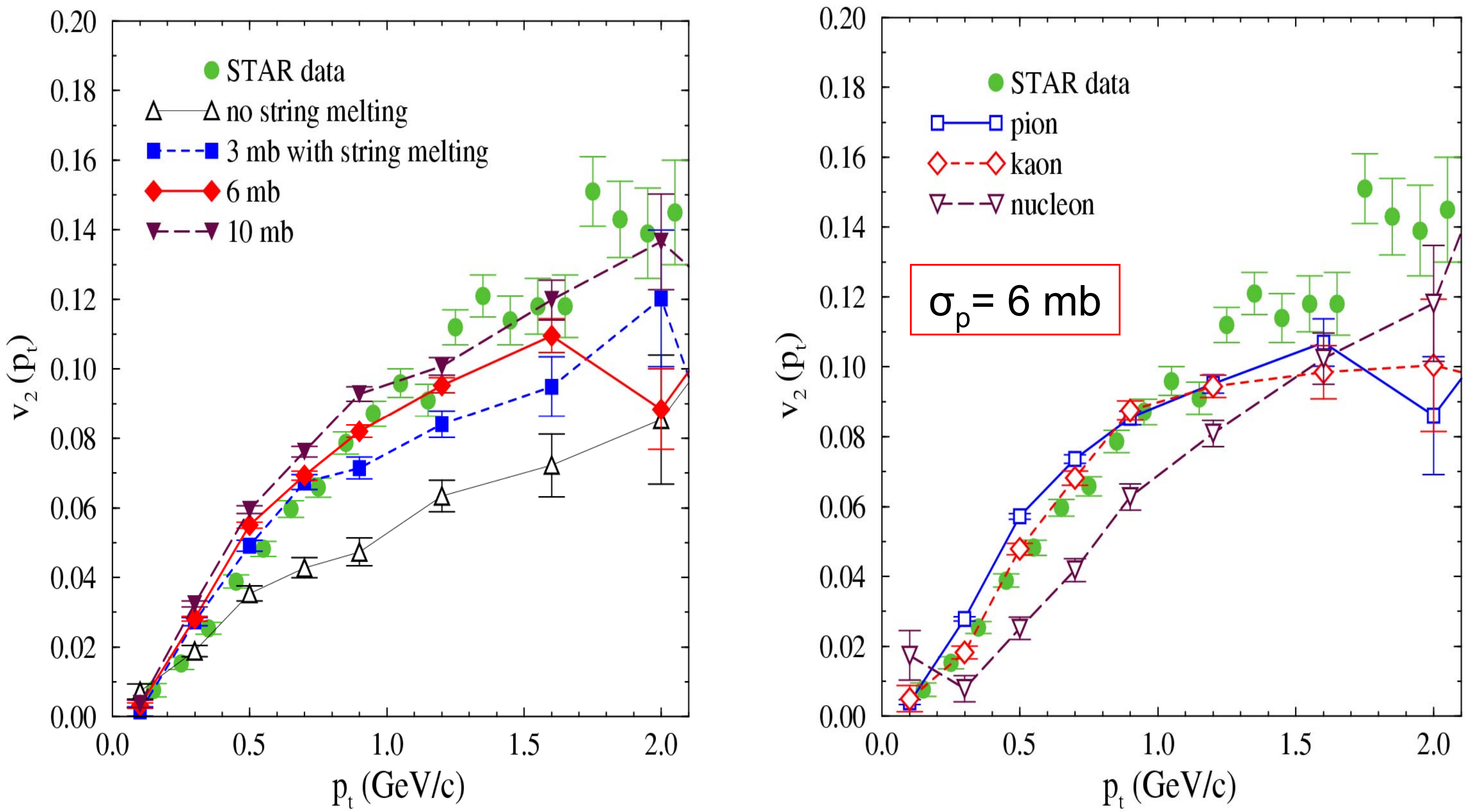

- Need string melting and large parton scattering cross section
- Mass ordering of v_2 at low p_T as in hydrodynamic model

Valence quark number scaling of hadron elliptic flow

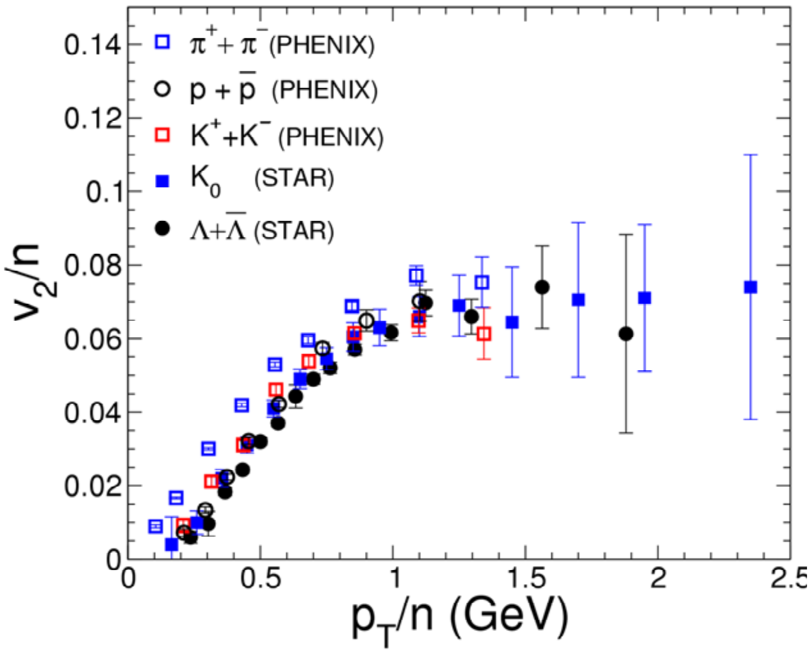

Quark number scaling:

$$\boxed{\frac{1}{n} v_2(p_T / n)}$$

same for mesons and baryons except pions which are mainly from resonance decays (Greco & Ko, PRC 70, 024901 (04))

Kolb, Chen, Greco & Ko, PRC 69, 051901 (04)

Naïve quark coalescence model:
Only quarks of same momentum can coalesce or recombine.

Quark transverse momentum distribution

$$\boxed{f_q(p_T) \propto 1 + 2 v_{2,q}(p_T) \cos(2\varphi)}$$

Meson elliptic flow

$$\boxed{v_{2,M}(p_T) = \frac{2 v_{2,q}(p_T/2)}{1 + 2 v_{2,q}^2(p_T/2)} \approx 2 v_{2,q}(p_T/2)}$$

Baryon elliptic flow

$$\boxed{v_{2,B}(p_T) = \frac{3 v_{2,q}(p_T/3)}{1 + 6 v_{2,q}^2(p_T/3)} \approx 3 v_{2,q}(p_T/3)}$$

Puzzle: Large proton/meson ratio

PHENIX, nucl-ex/0304022

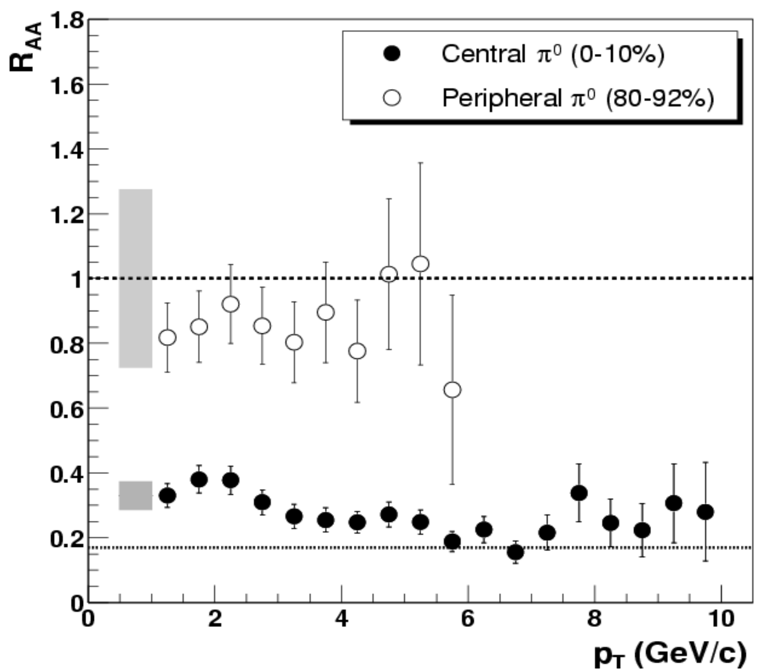

$$R_{AA} = \frac{dN_{Au+Au}}{\langle N_{bin} \rangle dN_{p+p}}$$

π^0 suppression: evidence of jet quenching before fragmentation

PHENIX, nucl-ex/0212014

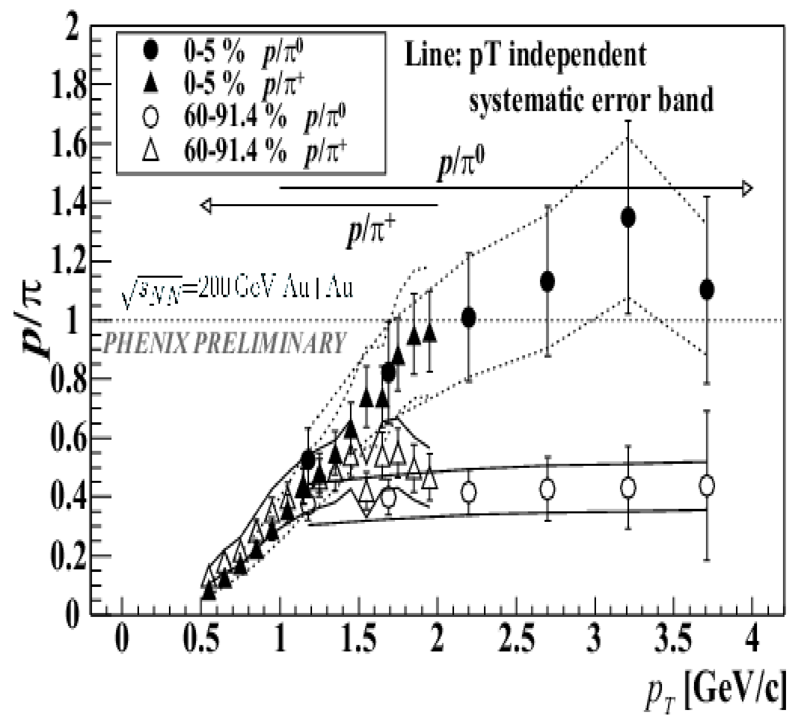

- Fragmentation leads to p/π ~ 0.2
- Jet quenching affects both
- Fragmentation is not the dominant mechanism of hadronization at p_T < 4-6 GeV

Large proton to pion ratio

Quark coalescence or recombination can also explain observed large p/pi ratio at intermediate transverse momentum in central Au+Au collisions.

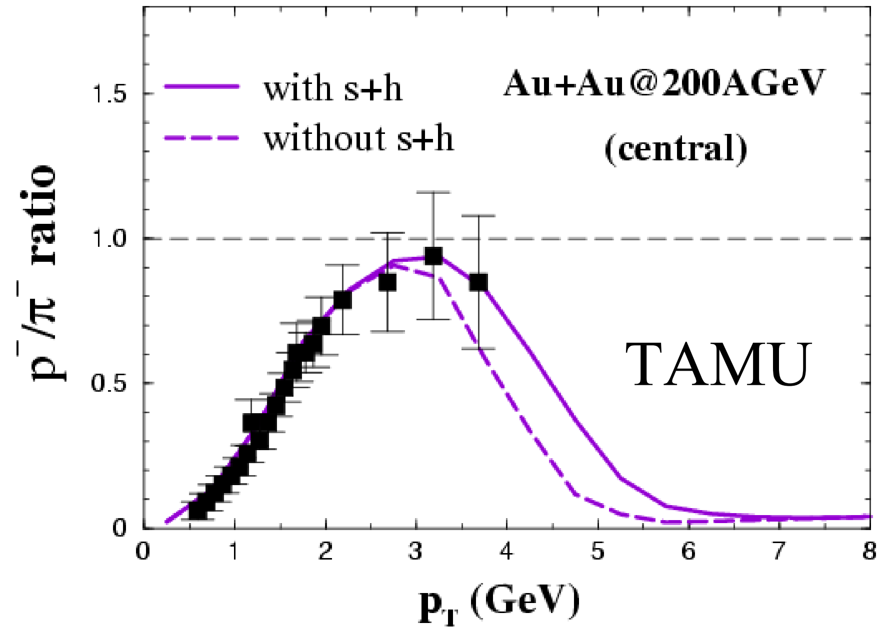

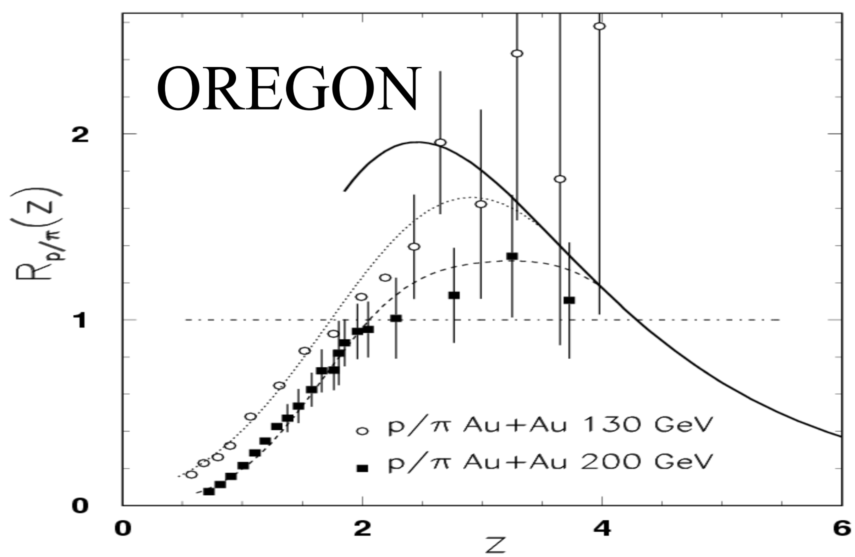

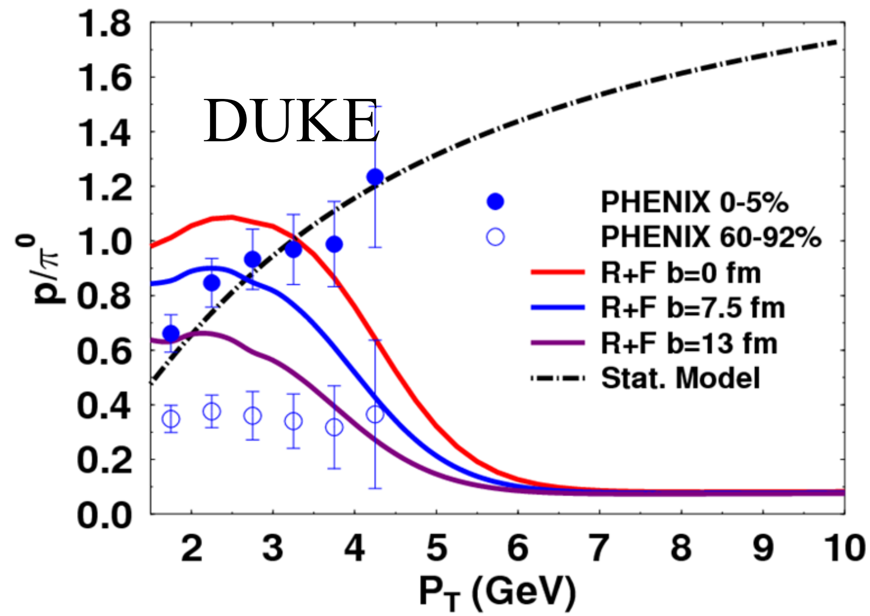

High P_T hadron suppression

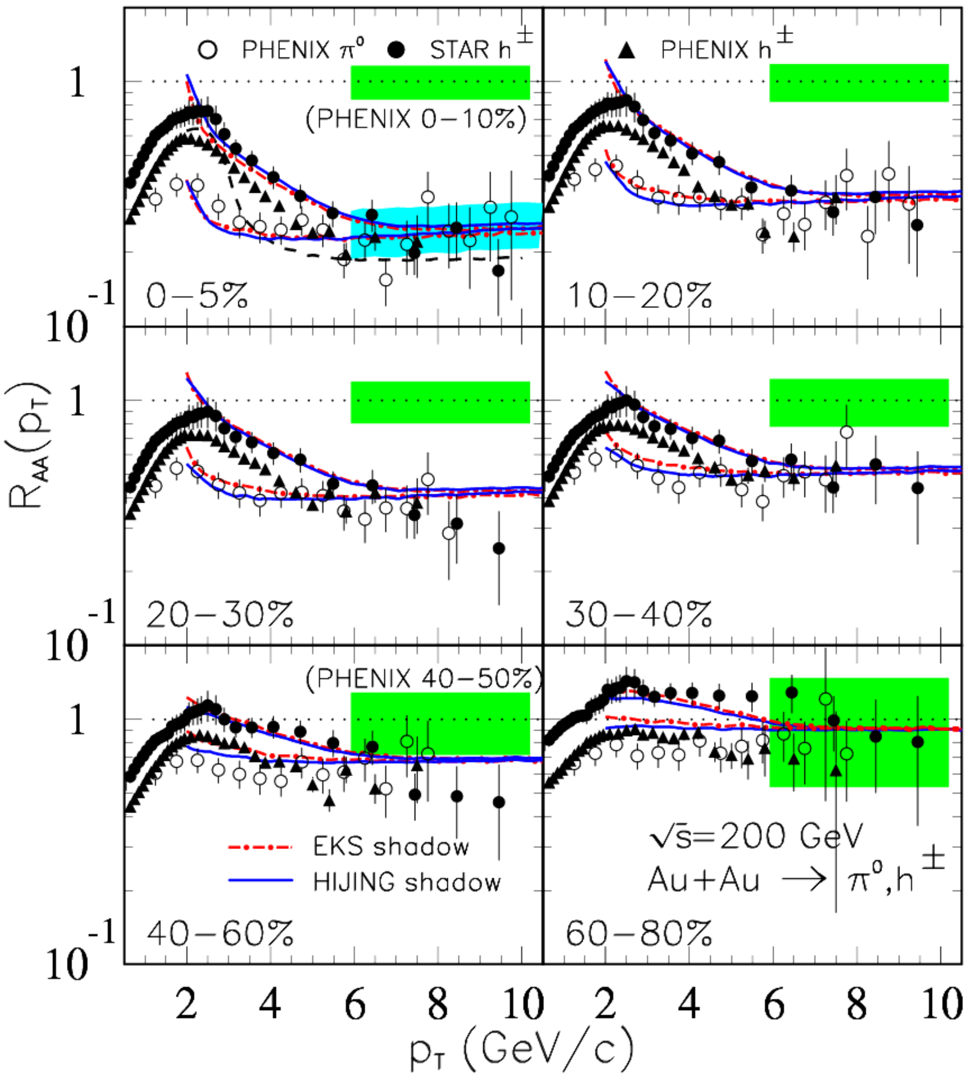

$$R_{AA} = \frac{dN_{Au+Au}}{\langle T_{AA} \rangle d\sigma_{p+p}}$$

Gyulassy, Levai & Vitev, PRL 85, 5535 (00)

Wang & Wang, PRL 87, 142301 (01)

Parton energy loss due to radiation

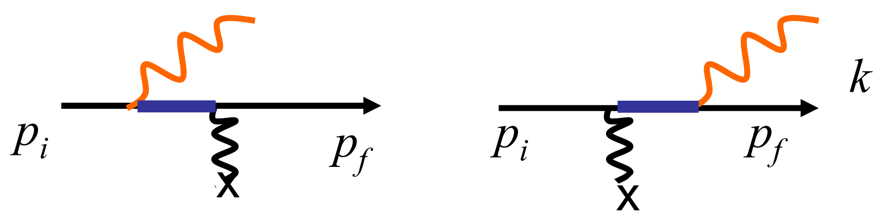

Jet quenching → initial energy density → 5-10 GeV/fm^3

Charm R_{AA} and elliptic flow from AMPT

Zhang, Chen & Ko, PRC 72, 024906 (05)

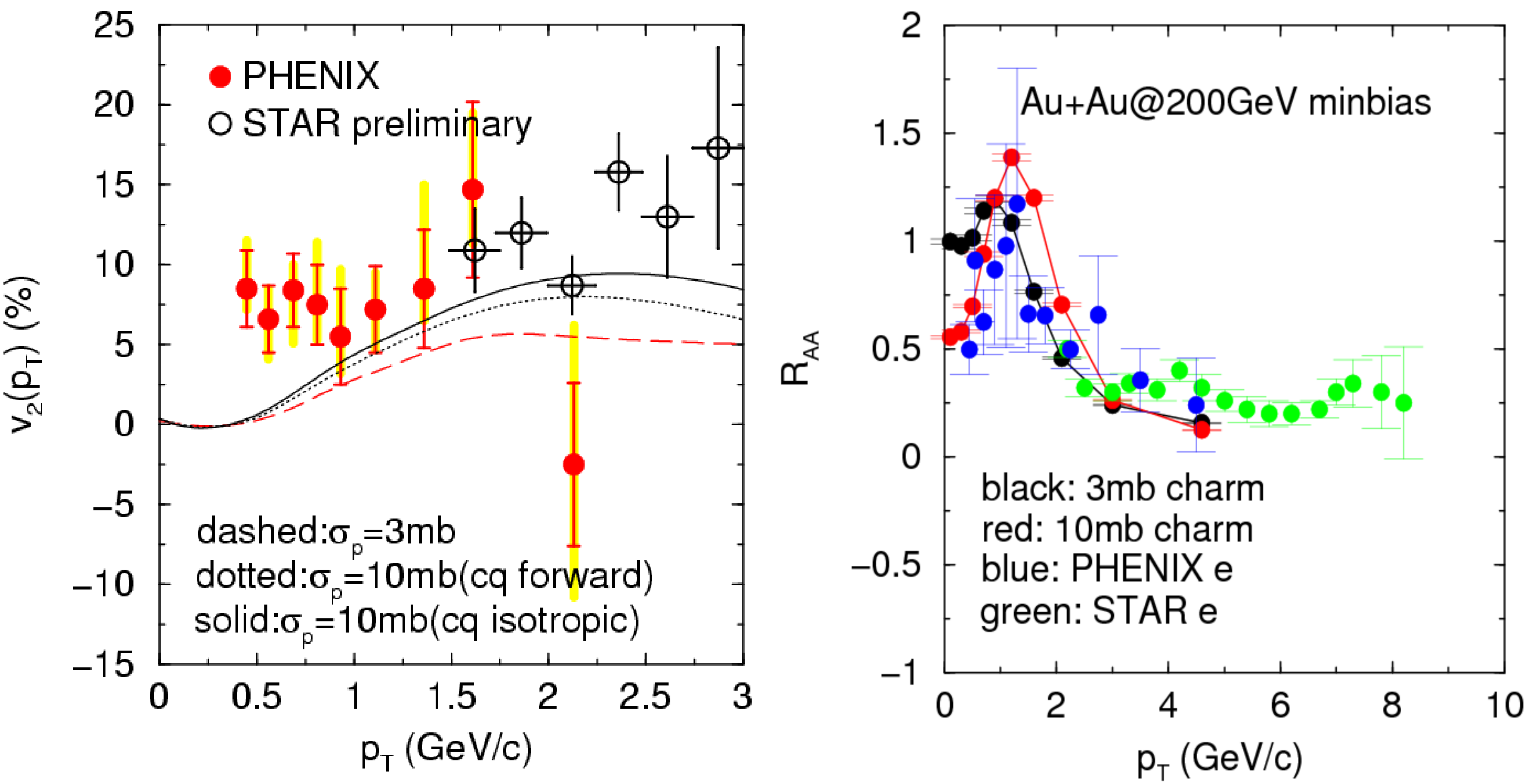

- Need large charm scattering cross section to explain data.
- Smaller charmed meson elliptic flow is due to use of current light quark masses in ZPC.

Heavy quark energy loss in pQCD

a) Radiative energy loss (Amesto *et al.,* PLB 637, 362 (2006))

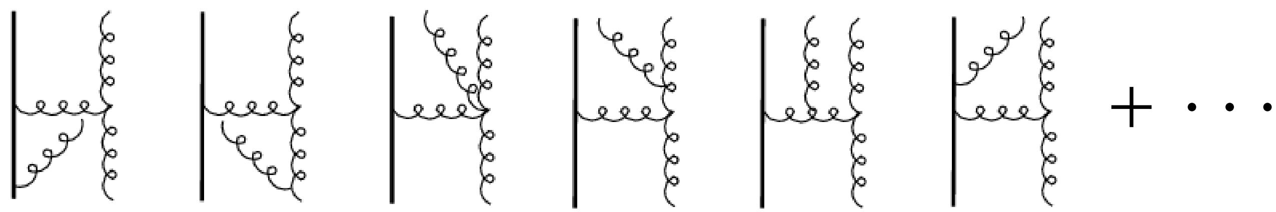

b) Radiative and elastic energy loss (Wicks *et al.,* NPA 784, 426 (2007))

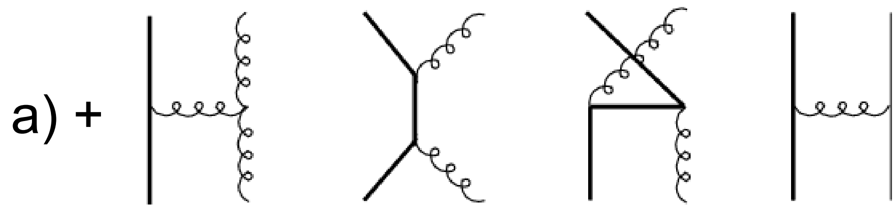

c) Three-body elastic scattering (Liu & Ko, JPG 34, S775 (2007))

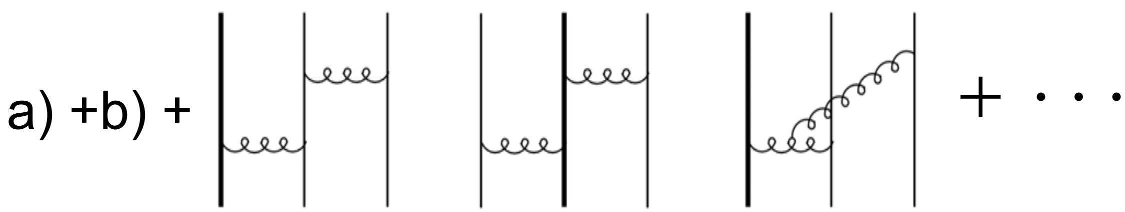

- May be important as interparton distance ~ range of parton interaction
- At T=300 MeV, $N_g \sim (N_q + N_{qbar}) \sim 5/fm^3$, so interparton distance ~ 0.3 fm
- Screening mass $m_D = gT \sim 600$ MeV, so range of parton interaction ~ 0.3 fm

Spectrum and nuclear modification factor of electrons from heavy meson decay

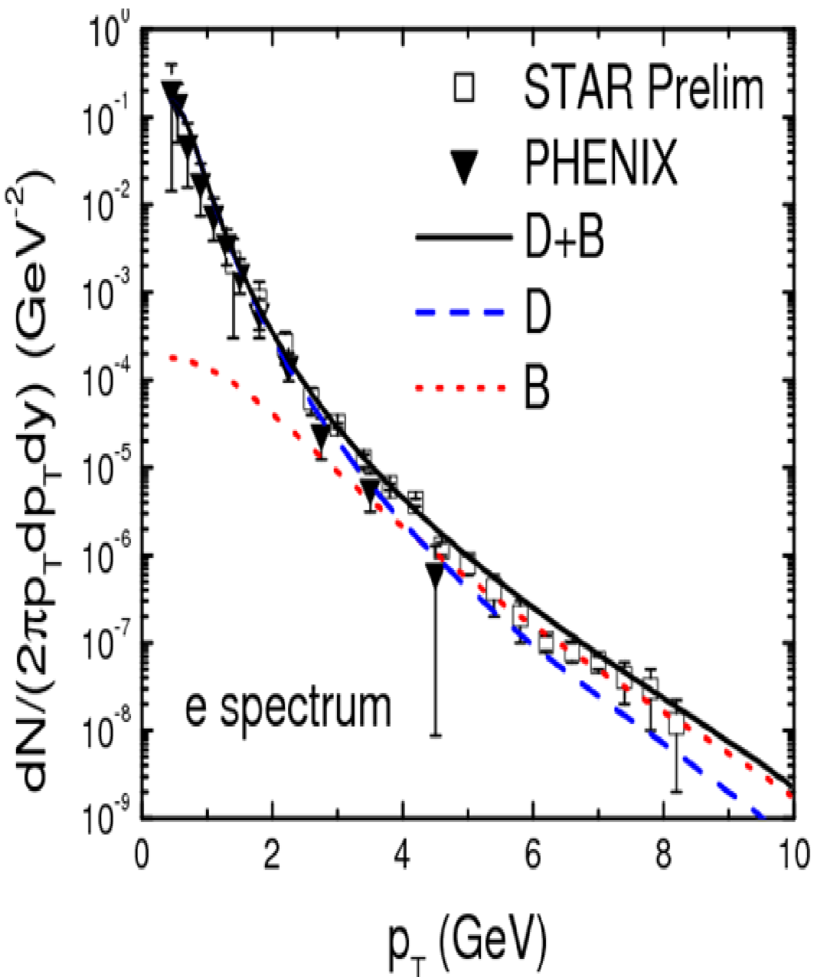

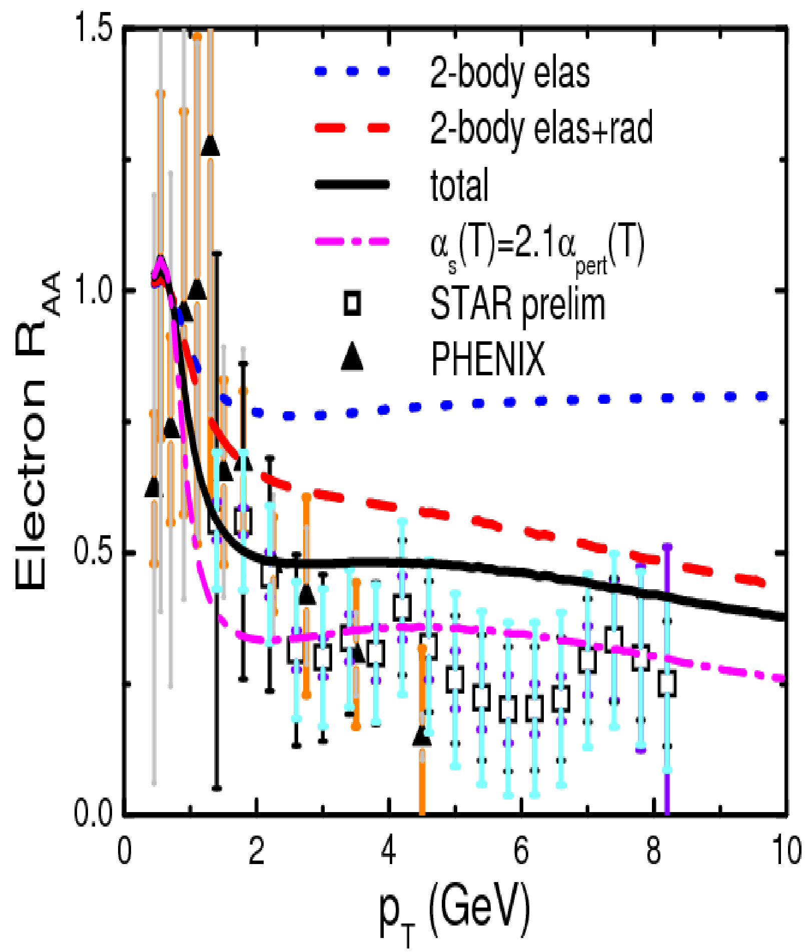

Reasonable agreement with data from Au+Au @ 200A GeV after including heavy quark three-body scattering and increasing α_s by 2.

Resonance effect on charm scattering in QGP

Van Hees & Rapp, PRC 71, 034907 (2005)

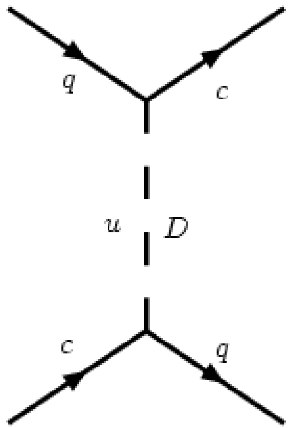

$$\sigma_{c\bar{q}\to c\bar{q}} = \frac{1}{9}\frac{2J+1}{4}\frac{\pi}{k^2}\frac{\Gamma_D^2}{\left(s^{1/2} - m_D\right)^2 + \Gamma_D^2/4}$$

With $m_c \approx 1.5$ GeV, $m_q \approx 5$-10 MeV, $m_D \approx 2$ GeV, $\Gamma_D \approx 0.3$-0.5 GeV, and including scalar, pseudoscalar, vector, and axial vector D mesons gives

$$\sigma_{cq\to cq}(s^{1/2}=m_D) \approx 6 \text{ mb}$$

Since the cross section is isotropic, the transport cross section is 6 mb, which is about 4 times larger than that due to pQCD t-channel diagrams, leading to a charm quark drag coefficient $\gamma \sim 0.16$ c/fm in QGP at T=225 MeV.

Van Hees, Greco, and Rapp, PRC 73, 034913 (2006)

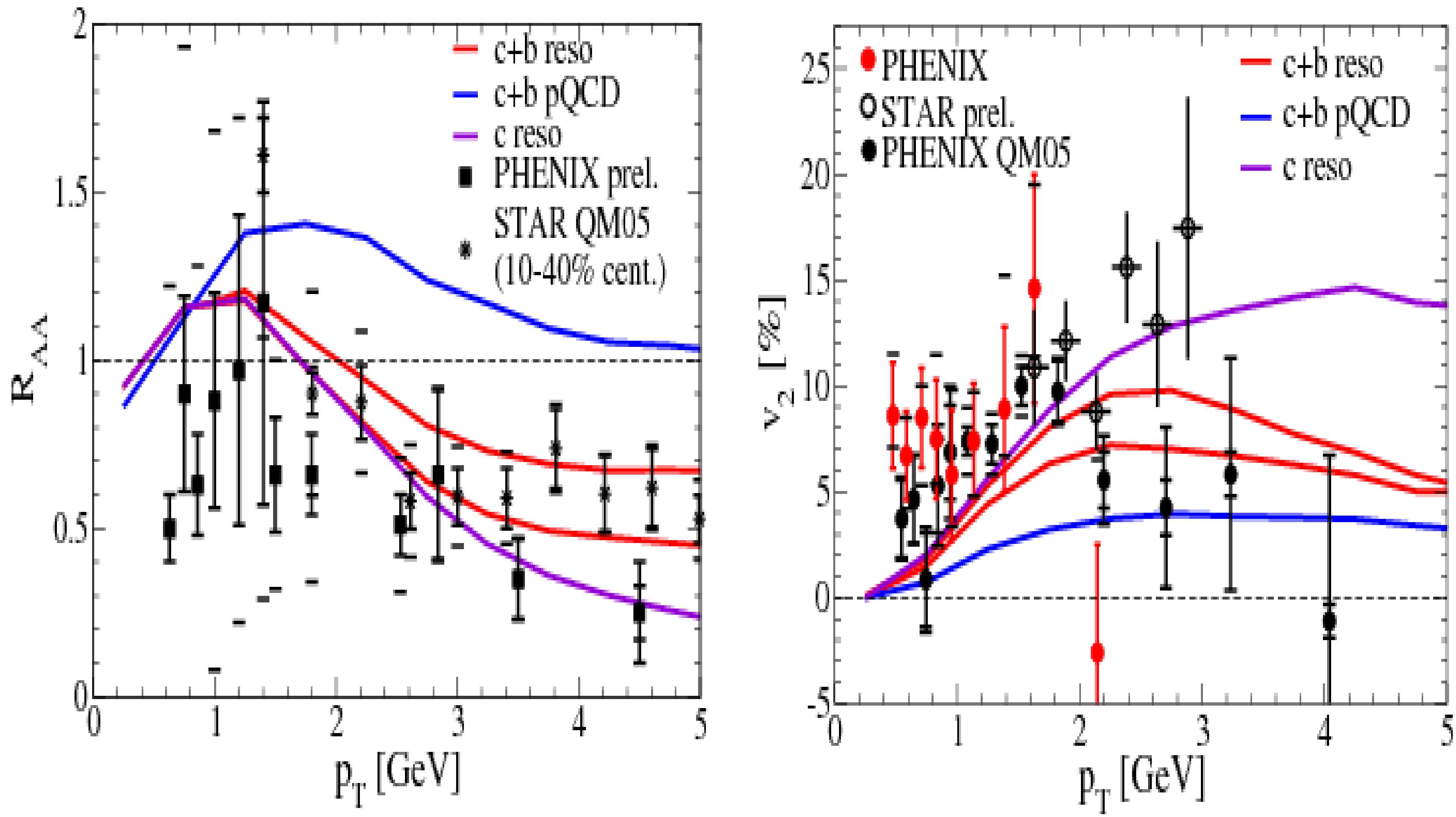

Langevin simulation with resonance scattering and including both coalescence and fragmentation can explain the data

Static potentials from lattice QCD

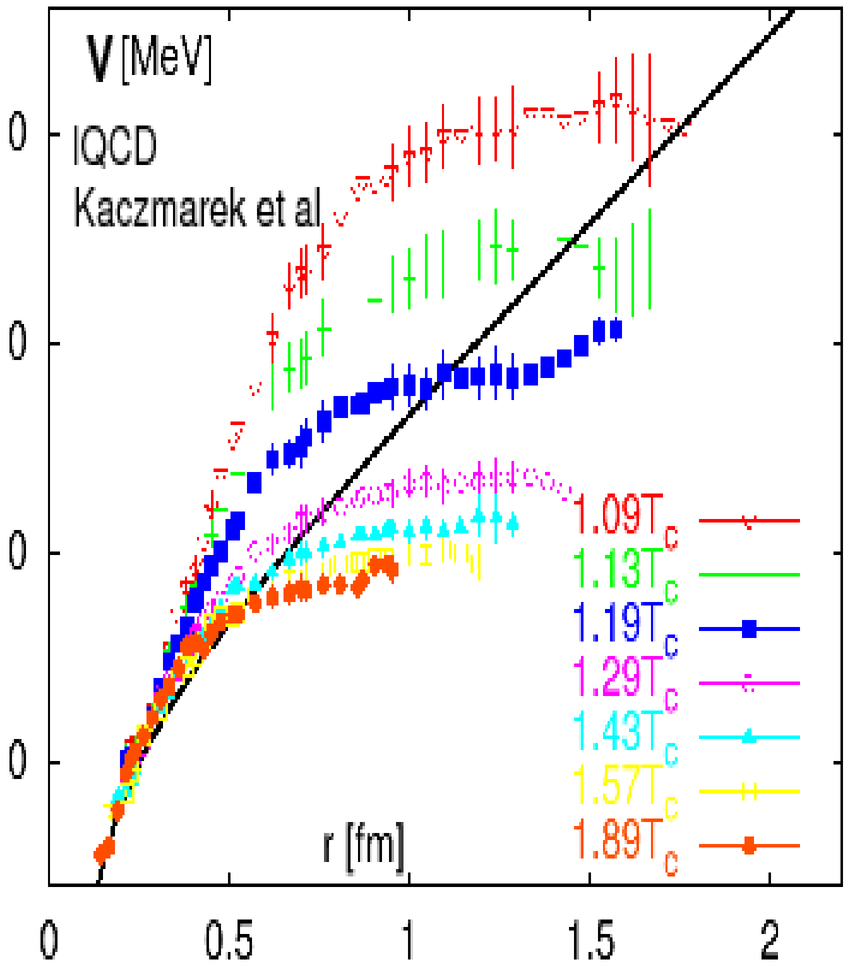

Internal energy

$$U_1(r,T) = F_1(r,T) - T\,\frac{\partial F_1(r,T)}{\partial T}$$

Color singlet potential

$$V_1(r,T) = U(r,T) - U(\infty,T)$$

Color triplet potential

$$V_3(r,t) = \frac{V_1(r,T)}{2}$$

Scattering matrix of quark and antiquark in QGP

Cabrera and Rapp, PR D 76, 114506 (2007)

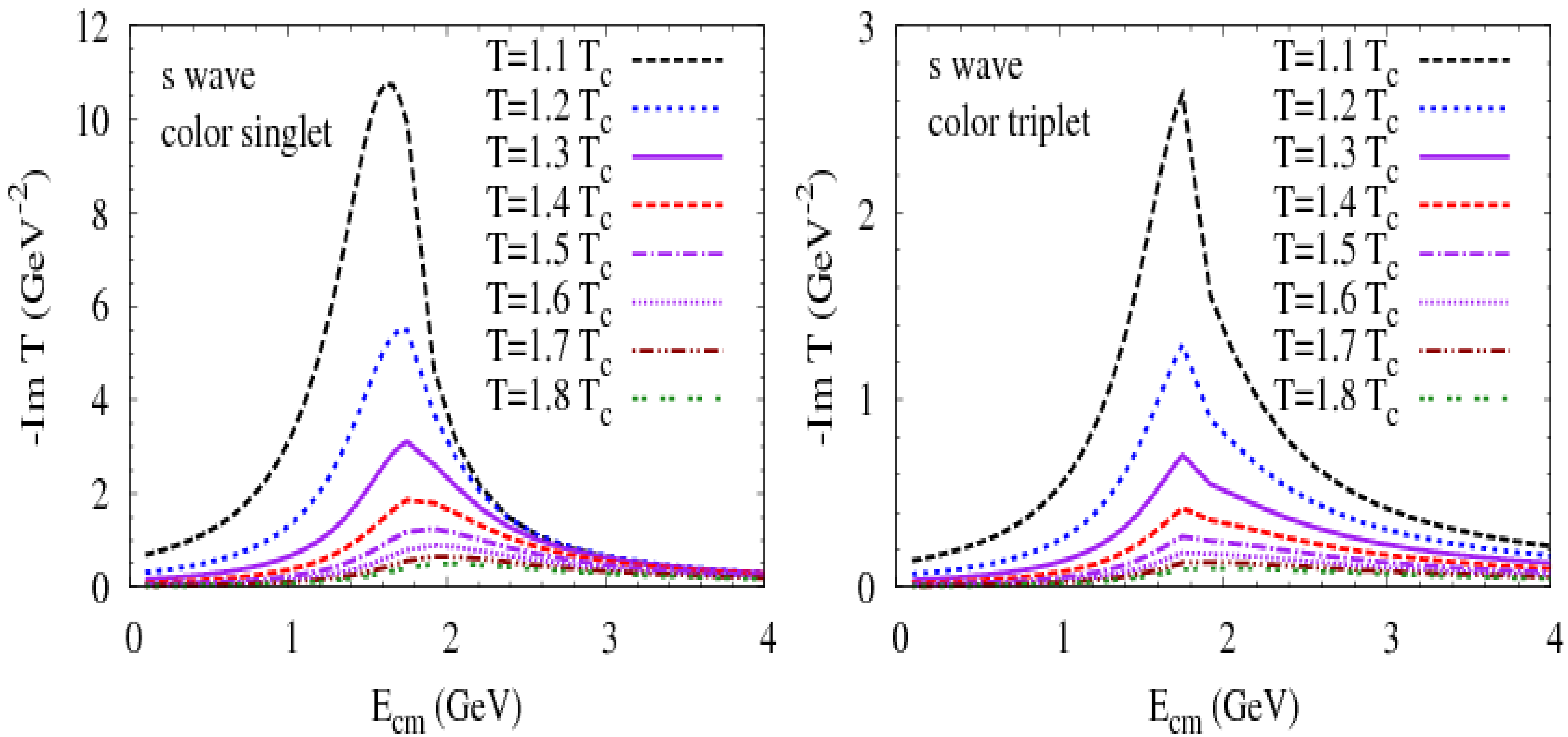

- Obtained by solving Lippmann-Schwinger equation for c-qbar
- Resonance formation at T close to T_c

Charm suppression at FAIR

Liu & Ko (2007)

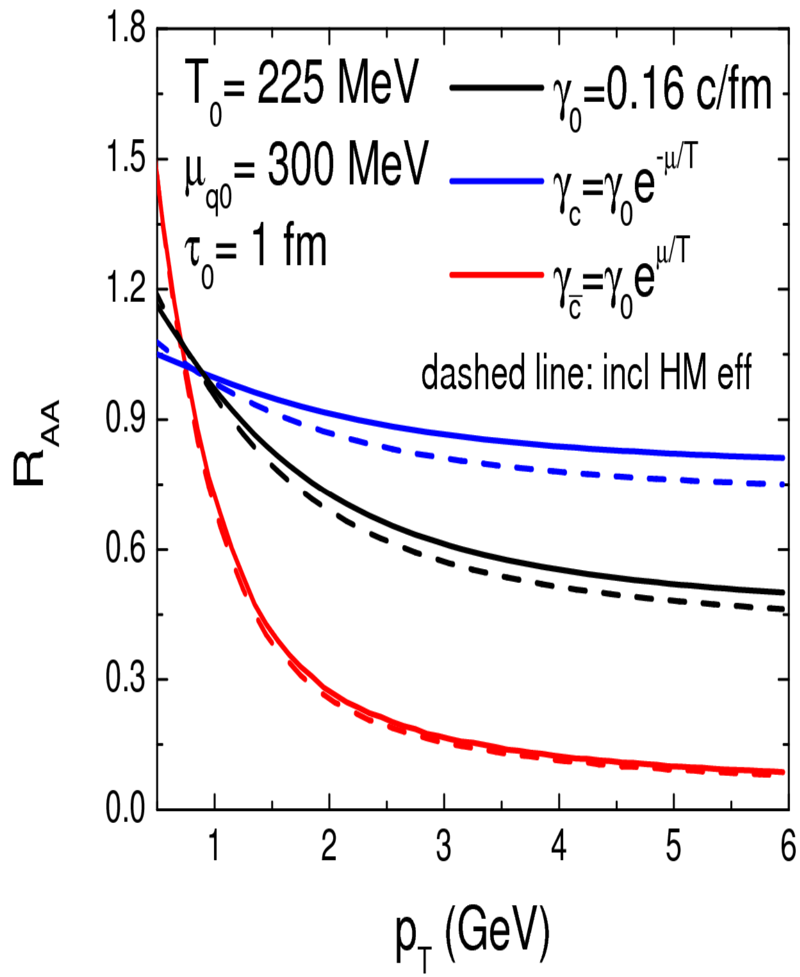

$$R_{AA} = \frac{dN_{Au+Au}}{\langle T_{AA} \rangle d\sigma_{p+p}}$$

- dN_{Au+Au}= differential heavy flavor yield in Au+Au collisions
- $d\sigma_{p+p}$= corresponding differential cross section in p+p collisions
- $<T_{AA}>$= nuclear overlap integral

- pQCD gives similar c and cbar cross sections in QGP, irrespective to the baryon chemical potential (solid line).
- Resonance scattering leads to different c and cbar cross sections in QGP with finite baryon chemical potential (blue and red lines)

Conclusions

- Heavy ion collisions have made it possible to learn about the properties of dense nuclear matter

  - At high energies → isoscalar incompressibility K~ 210-300 MeV

  - With neutron-rich nuclei → $E_{sym}(\rho)$~ 32 $(\rho/\rho_0)^{\gamma}$ with $0.7<\gamma<1.1$

    for $\rho<1.2\rho0$ → $K_{asy}(\rho_0)$~-550 ± 50 MeV and L~ 88 ± 25

  - At ultrarelativistic energies → a strongly coupled quark-gluon plasma

- Future radioactive beam facilities → Nuclear symmetry energy at high densities

- Experiments at LHC and future FAIR allow to probe QGP at even higher temperature and finite baryon chemical potential, respectively